Non-Fermi-liquid aspects of cold and dense QED and QCD: Equilibrium and nonequilibrium

D. Boyanovsky
Department of Physics and Astronomy, University of Pittsburgh, Pittsburgh, Pennsylvania 15260 and LPTHE, Université Pierre et Marie Curie (Paris VI) et Denis Diderot (Paris VII), Tour 16, 1er. étage, 4, Place Jussieu, 75252 Paris, Cedex 05, France

H. J. de Vega
LPTHE, Université Pierre et Marie Curie (Paris VI) et Denis Diderot (Paris VII), Tour 16, 1er. étage, 4, Place Jussieu, 75252 Paris, Cedex 05, France and Department of Physics and Astronomy, University of Pittsburgh, Pittsburgh, Pennsylvania 15260

(Received 14 September 2000; published 11 January 2001)

We study equilibrium and nonequilibrium aspects of the *normal* state of cold and dense QCD and QED. The exchange of dynamically screened magnetic gluons (photons) leads to infrared singularities in the fermion propagator for excitations near the Fermi surface and the breakdown of the Fermi liquid description. We implement a resummation of these infrared divergences via the Euclidean renormalization group to obtain the spectral density, dispersion relation, widths, and wave function renormalization for single quasiparticles near the Fermi surface. We find that all features scale with anomalous dimensions: $\omega_p(k)\propto|k-k_F|^{1/(1-2\lambda)}$, $\Gamma(k)\propto|k-k_F|^{1/(1-2\lambda)}$; $Z_p(k)\propto|k-k_F|^{2\lambda/(1-2\lambda)}$ with $\lambda=\alpha/6\pi$ for QED, $(\alpha_s/6\pi)(N_c^2-1)/2N_c$ for QCD with N_c colors and N_F flavors. The discontinuity of the quasiparticle distribution at the Fermi surface vanishes. For $k\approx k_F$ we find $n_{k\approx k_F}=\sin[\pi\lambda]/2\pi\lambda-(k-k_F)/\pi M(1-4\lambda)+\mathcal{O}(k-k_F)^2$ with M the dynamical screening scale of magnetic gluons (photons). The dynamical renormalization group is implemented to study nonequilibrium relaxation. The amplitude of single quasiparticle states with momentum near the Fermi surface falls off as $|\Psi_{k\approx k_F}(t)|\approx|\Psi_{k\approx k_F}(t_0)|e^{-\Gamma(k)(t-t_0)}[t_0/t]^{2\lambda}$. Thus quasiparticle states with Fermi momentum have zero group velocity and relax with a power law with a coupling-dependent anomalous dimension.

DOI: 10.1103/PhysRevD.63.034016 PACS number(s): 12.38.Mh, 11.15.Bt, 12.38.Aw, 12.38.Lg

I. INTRODUCTION AND MOTIVATION

There is a substantial theoretical and experimental effort to map the phase diagram of QCD as a function of temperature (T) and chemical potential (μ). Current theoretical ideas suggest [1] that heavy ion collision experiments from SIS to the BNL Alternating Gradient Synchrotron (AGS), CERN Super Proton Synchrotron (SPS), BNL Relativistic Heavy Ion Collider (RHIC), and finally the CERN Large Hadron Collider (LHC) have the potential to study the region of the phase diagram for $T\leqslant 300$–400 MeV and $\mu\leqslant 0.6$ GeV with higher (T) and lower (μ) for RHIC and LHC. Understanding this region of the phase diagram can provide insight into the QCD phase transition in the early Universe, about 10 μs after the big bang, as well as the equation of state of hot and dense QCD. Matter at low temperature $\leqslant 10$ MeV and up to nuclear matter density $\rho_0\approx 0.16$ fm^{-3}, $\mu\approx 300$ MeV is amenable to study by low energy nuclear systems such as multifragmentation phenomena in nuclei. Cold and dense nuclear matter for densities larger than a few times the nuclear matter density cannot be studied with terrestrial accelerators and is the realm of astrophysical compact objects, such as neutron stars [2,3]. The fascinating possibility of detecting a phase transition in quark matter in neutron star x-ray binaries was raised recently [4,5], where the signal would be a pronounced peak in the frequency distribution of x-ray neutron stars due to a long spin-up stage and the cooling history as revealed by the (soft) x-ray spectra [22–24]. Thus while QCD at high temperature and relatively small chemical potential can be experimentally studied with ultrarelativistic heavy ion collisions, astrophysical observation of the properties of neutron stars can provide observable signatures from cold and dense QCD if quark matter is the correct description of the core of spinning neutron stars.

While there is a substantial body of results on QCD at finite temperature on the lattice, the lack of a manifest reality of the fermion determinant with finite chemical potential presents a problem for the lattice program with the important exception of two colors which have received considerable attention recently [6–8].

An important aspect of QCD at large chemical potential is that of color superconductivity [9] which arises from a paring instability of the free Fermi gas in the color antitriplet channel. Since the original proposal of color superconductivity via a one (screened) gluon exchange [9], there has been an increased interest in color superconductivity [10–20] and diquark condensation [21]. The presence of diquark condensates in the cold and dense core of neutron stars could have potential observable signatures in their cooling history as well as in the magnetic fields of pulsars [22–24]. Therefore the study of cold and dense QCD is warranted by a definite phenomenological and observable impact if not on terrestrial accelerator experiments certainly in the astrophysical signatures of neutron stars [25].

Goals. The common framework to study degenerate correlated fermion systems is that of Fermi liquid theory (see next section). The emergence of superconductivity (diquark condensation in the case of QCD) is associated with the instability of the normal Fermi liquid towards an attractive pairing interaction. In the case of a weakly interacting Fermi

system the starting point is the free Fermi gas and pairing results in the opening of a gap in the single particle spectrum at the Fermi surface. Fermi liquid theory is argued to describe the low energy effective field theory of nuclear matter [26] and is therefore an important tool to study nuclear matter and its impact in astrophysical compact objects.

Recently it has been argued, within the context of color superconductivity, that the exchange of dynamically screened (via Landau damping) magnetic gluons results in strong infrared divergences that lead to the breakdown of the Fermi liquid description of cold and dense QCD in perturbation theory [27]. A similar situation was found in the case of a nonrelativistic electron gas with magnetic interactions [28–30], where it was argued that there would be no observable consequences of the breakdown of Fermi liquid theory for *terrestrial densities*.

While diquark condensation and color superconductivity in its various forms have been studied extensively in the literature, we are aware of only one previous study of non-Fermi-liquid aspects of cold and dense QCD [27], which revealed large corrections to the superconducting gap [27]. Further corrections to the superconducting gap were found from lifetime effects [31] not associated with the breakdown of Fermi liquid theory.

Studying Fermi liquid aspects of the *normal* phase is an important part of the program towards understanding cold and dense QCD. As mentioned above, understanding the properties of the normal phase is perhaps the first step towards a complete assessment of the pairing instabilities and properties of the superconducting state. Furthermore, if the pairing interaction opens a gap at the Fermi surface of *some* quarks, such as the two or three color superconducting phases (2SC or 3SC) [10–16,20,25], the remaining gapless quarks will be described by the concomitant Fermi liquid.

Our goal in this article is to provide a comprehensive study of non-Fermi-liquid aspects in the *normal* phase of cold and dense QCD, postponing to a forthcoming article the study of the implications of the breakdown of Fermi liquid theory on color superconductivity. While the study in [27] focused on the corrections to the color superconducting gap and issues of gauge invariance, we study both equilibrium and nonequilibrium aspects of the non-Fermi-liquid behavior. In particular we focus on (i) the dispersion relation and damping rates of quasiparticles near the Fermi surface, as these reveal anomalous dimensions resulting from the breakdown of Fermi liquid theory, and (ii) the relaxation of these quasiparticles: again we find anomalous relaxation with the origin in the same infrared divergences responsible for the breakdown of Fermi liquid theory. Our main motivations for initiating this study and long term goals are manifold: (a) to obtain a further assessment of non-Fermi-liquid corrections to the superconducting gaps, critical temperature, and spectrum of excitations in the superconducting phase, (b) a study of the potential implications of non-Fermi-liquid corrections to the neutrino emissivity and the cooling rate of neutron stars with degenerate quark-matter cores, (c) a more complete and detailed understanding of the properties of dense QCD in a regime which is not yet amenable to lattice simulations, and (d) a study of transport phenomena in the non Fermi liquid, which is relevant to cooling and thermodynamics of neutron stars.

In this article we begin this program by studying in detail the breakdown of the Fermi liquid description and by providing a comprehensive analysis of the spectrum of single quasiparticle excitations in the *normal* phase along with their relaxation properties.

Strategy. We study both QED and QCD at zero temperature but large (baryon) density so that a perturbative analysis is reliable. In this regime the hard-dense-loop (HDL) approximation, which is the finite density equivalent of the hard-thermal-loop program of Braaten and Pisarski for finite temperature [32–37], is reliable and describes the main aspects of the static and dynamical screening of gluons (and photons). The leading order in the HDL approximation is the *same* in Abelian (QED) and non-Abelian (QCD) theories and the screening of gauge fields is completely determined by the one loop quark polarization at finite (and large) density [34–37]. In this approximation, static ''longitudinal'' gluons (instantaneous Coulomb interaction) are screened by a Debye screening mass $m_D \propto g\mu$ while transverse gluons are only *dynamically* screened via Landau damping [32,33]. To this order in the HDL approximation the polarization tensor for gluons in QCD is similar to that for photons in QED save for trivial color and flavor factors. The main difference between QCD and QED in this approximation is that while one gluon exchange leads to an attractive (pairing) interaction in the antitriplet particle-particle channel and therefore to diquark condensation, there is no such attractive channel in QED.[1] Thus, to this order in the HDL approximation, the Fermi liquid aspects of the normal state of cold and dense QCD are similar to those of QED. Thus we present our study within the framework of QED which, accounting for the trivial color and flavor factors, also describes those of the normal state of QCD to leading order in the HDL approximation.

As described in detail in Sec. II, a Fermi liquid description has an associated ''order parameter''; this is the jump discontinuity of the Fermi distribution function (of the interacting) system at the Fermi momentum. This discontinuity is given by the residue (wave function renormalization) of the quasiparticle pole for quasiparticles with the Fermi momentum. The breakdown of the Fermi liquid picture is associated with the vanishing of this order parameter; i.e., the Fermi distribution function is *continuous* at the Fermi momentum. We begin by obtaining the quark propagators to leading order in the HDL approximation, corresponding to one bare gluon exchange in the quark self-energy, and show explicitly that to this order there is a sharp discontinuity at the Fermi surface determined by the wave function renormalization of the quasiparticle pole.

However, this picture does not survive screening corrections to the gluon propagator; whereas longitudinal gluon exchange leads to an infrared finite contribution, the ex-

[1]However, we expect the Overhauser effect to be present in QED [19], i.e., particles above and holes below the Fermi surface bound by their mutual (screened) Coulomb attraction. These are the counterpart of exciton bound states in condensed matter.

change of magnetic gluons which are only *dynamically* screened by Landau damping introduces logarithmic divergences in the quark propagator for quasiparticles near the Fermi surface.

For excitations with Fermi momentum we argue that these infrared divergences are similar to those of a critical theory at the upper critical dimensionality. Thus we provide a resummation of the quark propagator for particles with the Fermi momentum using the Euclidean renormalization group which reveals the emergence of anomalous dimensions in the spectral density. Nonequilibrium aspects are studied by implementing a dynamical renormalization group [38] which provides a resummation of the quark propagator *directly in real time*. The dynamical renormalization group reveals power law relaxation with anomalous dimension for quasiparticles with Fermi momentum.

Summary of the results. The exchange of dynamically screened magnetic gluons leads to infrared divergences in the single particle propagator for particle excitations near the Fermi surface. These divergences are akin to those found in critical phenomena for a critical theory at the upper critical dimensionality. We implement a resummation of the perturbative expansion via the Euclidean renormalization group. We find that the particle component of the quark propagator for excitations near the Fermi surface is a *scaling function* of the two variables $\tilde{\omega}=\omega-\mu$, $\tilde{k}=k-\mu$ with anomalous exponents that depend on the gauge coupling. For $\tilde{k}\neq 0$ the spectral density has the Breit-Wigner (quasiparticle) form, with the quasiparticle dispersion relation, width, and residue given, respectively, by

$$\omega_p(\tilde{k})\propto|\tilde{k}|^{1/(1-2\lambda)},\quad \Gamma(\tilde{k})\propto\sin[\pi\lambda]|\tilde{k}|^{1/(1-2\lambda)},$$
$$Z_p(\tilde{k})\propto|\tilde{k}|^{2\lambda/(1-2\lambda)}, \tag{1.1}$$

with the effective coupling given by

$$\lambda=\begin{cases}\dfrac{\alpha}{6\pi} & \text{for QED,}\\[2ex] \dfrac{\alpha_s}{6\pi}\dfrac{N_c^2-1}{2N_c} & \text{for QCD with } N_c \text{ colors and } N_F \text{ flavors.}\end{cases} \tag{1.2}$$

The residue of the quasiparticle pole vanishes as $k\to k_F$, leading to the following form of the (quasi)particle distribution function near the Fermi surface:

$$n_{k\approx k_F}=\frac{\sin[\pi\lambda]}{2\pi\lambda}-\frac{\tilde{k}}{\pi M(1-4\lambda)}+\mathcal{O}(\tilde{k})^2,$$
$$M=\begin{cases}\dfrac{g\mu}{2\pi} & \text{for QED,}\\[2ex] \dfrac{g\mu}{2\pi}\dfrac{N_F}{2} & \text{for QCD with } N_F \text{ flavors,}\end{cases} \tag{1.3}$$

revealing the vanishing of the discontinuity of the Fermi distribution function at the Fermi surface and therefore the vanishing of the Fermi liquid order parameter.

Implementing a real-time, i.e., a dynamical version of the renormalization group to study the nonequilibrium relaxation of single quasiparticles near the Fermi surface, we find that the amplitude of the wave function of single quasiparticle states near the Fermi surface fall off as

$$|\psi_{k\approx k_F}(t)|\propto|\psi_{k\approx k_F}(t_0)|\ e^{-\Gamma(\tilde{k})(t-t_0)}\left[\frac{t_0}{t}\right]^{2\lambda}. \tag{1.4}$$

Thus quasiparticles with Fermi momentum have vanishing group velocity and relax with an anomalous power law.

We make a comparison between these features of cold and dense QCD (and QED) and those of strongly correlated quasi-one-dimensional Fermi systems that feature non-Fermi liquid behavior and are described as Luttinger liquids [39,40].

The article is organized as follows: in Sec. II we summarize the aspects of Fermi liquids that are relevant for our discussion. In Sec. III we obtain the expression for the quasiparticle distribution function in terms of the quark spectral density and obtain the equation of motion for quarks which will be used to study nonequilibrium aspects. In Sec. IV we study the equilibrium aspects of single quasiparticles. We begin by studying the quark propagator to lowest order in the HDL approximation, i.e., with the self-energy given by the exchange of hard (bare) gluons, and make contact with the Fermi liquid description to this order. Soft ($q<g\mu$) gluons require HDL resummation, and the propagator for particles near the Fermi surface is computed by including HDL (screening) corrections to the exchanged gluon. The resulting infrared divergences are recognized to be similar to those of a critical theory at its upper critical dimension and resummed using the Euclidean renormalization group. The renormalization group improved spectral density features scaling behavior that leads to the single quasiparticle dispersion relation and lifetime that scales with anomalous dimensions. We show that the jump discontinuity of the single particle distribution function vanishes at the Fermi surface as a consequence of the vanishing of the single quasiparticle residue at the Fermi momentum. Section V explores nonequilibrium aspects: the relaxation of single quasiparticle excitations near the Fermi surface. Implementing a real-time version of the renormalization group reveals that single quasiparticle states

with Fermi momentum relax with a power law with anomalous dimension. In Sec. VI we summarize the connection between QED and the normal state of QCD to the order studied and address the important issue of vertex corrections. Our conclusions are discussed in Sec. VII. In this section we also discuss the striking resemblance of the spectral density and relaxation to that obtained in a Luttinger liquid [39,40] and some related conjectures on the non-Fermi-liquid aspects of high T_c superconductivity; we elaborate on the potential impact of the results and discuss their range of validity. An appendix contains many of the technical details.

II. HIGHLIGHTS OF A FERMI LIQUID

The most successful description of interacting degenerate Fermi systems in the *normal* state, i.e., nonsuperconducting or superfluid is Fermi liquid theory. Landau's original formulation, largely phenomenological, has as the basic hypothesis a one-to-one correspondence between the eigenstates of the interacting and noninteracting systems. In this formulation the *quasiparticles* are obtained from the single particle states of the noninteracting system via an adiabatic switching-on of the perturbation [39–41]; hence for this picture to remain valid the interactions should not lead to phase transitions. The *Landau quasiparticle* concept is appropriate for excitations very near the Fermi surface, since for short range interactions the lifetime of these quasiparticles is $\tau \approx |k-k_F|^{-2}$ [39–41], which after including screening effects also holds in the case of Coulomb interactions [43]. For quasiparticles near the Fermi surface the adiabatic hypothesis is reasonable [39,40] and Landau's phenomenological theory is applicable to study transport phenomena of low energy excitations [41]. A more modern and consistent description of Fermi liquid theory is based on renormalization group ideas [44] which describe the low energy physics near the Fermi surface as fixed points of the renormalization group, and Fermi liquid interactions are those associated with marginal operators near this fixed point. This formulation of Fermi liquid theory reveals that the physics near the Fermi surface is very similar to that of critical phenomena and is completely determined by the gapless excitations associated with the formation of particle-hole states near the Fermi surface [44].

Fermi liquid theory is the starting point of a consistent study of the properties of degenerate, interacting Fermi systems; in particular BCS superconductivity can be understood as a result of the instability of the Fermi liquid towards pairing attractive interactions [45].

It has been adapted to study dense nuclear matter [26] and recently the renormalization group description of Fermi liquids has been extended to the interactions in field theory at nuclear matter density [46]. The conclusion of these studies is that Fermi liquid theory is an effective low energy theory for excitations near the Fermi surface. The field theoretical approach to Fermi liquids quantifies the main concepts of Fermi liquid theory in terms of the spectral density for the quasiparticles near the Fermi surface: a Breit-Wigner form with a small width (for $k \approx k_F$) and a finite residue at the ''quasiparticle pole,'' Z_{k_F}. The quasiparticle distribution function is distorted from the original Fermi-Dirac step function (at zero temperature) but a ''jump discontinuity'' remains at the Fermi surface which is determined by the wave function renormalization constant Z_{k_F} (see [47] for an explicit calculation in the electron gas). In a well-defined sense, this jump discontinuity is associated with an ''order parameter'' for a Fermi liquid [40,39]: a normal Fermi liquid corresponds to $Z_{k_F} \neq 0$ while for a non Fermi liquid $Z_{k_F}=0$. Transport properties of a degenerate Fermi gas depend on the renormalization of the (quasi)particles; for example, the coefficient of the linear power of temperature in the electronic specific heat is proportional to Z_{k_F}.

There are some notable examples of the breakdown of Fermi liquid theory such as the Kondo model of electrons interacting with magnetic impurities and ''quasi''-one-dimensional metals which provide a novel type of behavior for correlated electron systems: the Luttinger liquid (see [39,40] and references therein). This novel behavior of a correlated degenerate electron system is characterized by a vanishing jump at the Fermi surface and power law correlations akin to those found in critical phenomena [39].

Another system in which the Fermi liquid description breaks down is that of nonrelativistic electrons interacting via the exchange of ''magnetic'' (transverse) gauge bosons [28–30]. Recent conjectures suggest that this type of non-Fermi-liquid behavior [48] or ''Luttinger liquid'' behavior could explain the unusual properties of the normal phase of high temperature superconductors [49].

Our study of the normal state of cold and dense QCD (and of QED) reveals a striking resemblance with Luttinger liquid behavior; in particular, the renormalization group improved quark propagator that we find is remarkably similar to that proposed in [48,49] to describe the normal phase of high temperature superconductors.

III. PRELIMINARIES: QUASIPARTICLE DISTRIBUTION FUNCTION AND EQUATIONS OF MOTION

In this section we obtain the general expressions for the quasiparticle and quasiantiparticle distribution functions to make contact with Fermi liquid theory. The main aspect of the distribution function is that the existence of a jump discontinuity of the quasiparticle distribution at the Fermi momentum is the signal of Fermi liquid behavior. Furthermore, we obtain the effective equation of motion for the Dirac field in the medium to extract nonequilibrium aspects. Typically relaxation is studied by extracting the damping *rate* which is obtained from the imaginary part of the self-energy evaluated on the mass shell of the fermion and describes exponential relaxation. However, from the results of [34–37] it is found that the damping rate vanishes for quasiparticles with the Fermi momentum. However, the form of the fermion self-energy (see next section) strongly suggests the buildup of logarithmic infrared singularities just like in critical phenomena with the potential for summing up to a power law relaxation with anomalous dimensions. The solution of the real-time equation of motion resummed via the dynamical renormalization group will confirm power law relaxation

with anomalous dimension for single quasiparticles with the Fermi momentum. Thus in order to extract the correct relaxation behavior we must study the real-time evolution of the amplitude of the quasiparticle state which is obtained from the equation of motion.

A. Quasiparticle distribution function

The spatial Fourier transform of the Dirac field operator at any given time t can be written in the form

$$\psi(\vec{k},t)=\sum_s\ [b_{\vec{k},s}(t)U^{(s)}(\vec{k})+d^\dagger_{\vec{k},s}(t)V^{(s)}(-\vec{k})],\quad (3.1)$$

with $U^{(s)}(\vec{k})$, $V^{(s)}(\vec{k})$ the usual free particle Dirac spinors. We refer to the time-dependent operators $b_{\vec{k},s}(t)$ and $d^\dagger_{\vec{k},s}(t)$ as the annihilation and creation of quasiparticles and quasiantiparticles, respectively. Within the spirit of Fermi liquid theory, upon adiabatically switching on the interaction these operators interpolate between the free (bare) particles and the dressed (quasi)particles and antiparticles, respectively. We define the average number of quasiparticles and quasiantiparticles as

$$n_{\vec{k}}=\frac{1}{2}\sum_s\ \langle b^\dagger_{\vec{k},s}b_{\vec{k},s}\rangle,\quad (3.2)$$

$$\overline{n}_{\vec{k}}=\frac{1}{2}\sum_s\ \langle d^\dagger_{\vec{k},s}d_{\vec{k},s}\rangle,\quad (3.3)$$

where the expectation value is in the *exact* ground state, which is obtained from the unperturbed ground state by adiabatically switching on the perturbation from time $t\to-\infty$ to $t=0$. Using the properties of the usual spinor wave functions U,V and the results of the Appendix, it is straightforward to find

$$n_{\vec{k}}=\mathrm{Tr}\left\{\frac{\gamma_0(\not{K}+m)\gamma_0}{4\omega_{\vec{k}}}\langle\overline{\psi}(\vec{k},t)\psi(\vec{k},t)\rangle\right\}_{t=0}$$
$$=\mathrm{Tr}\left\{\frac{\gamma_0(\not{K}+m)\gamma_0}{4\omega_{\vec{k}}}[-iS^<_{\vec{k}}(t,t)]_{t=0}\right\},\quad (3.4)$$

$$\overline{n}_{\vec{k}}=\mathrm{Tr}\left\{\frac{(\not{K}-m)}{4\omega_{\vec{k}}}\langle\psi(\vec{k},t)\overline{\psi}(\vec{k},t)\rangle\right\}_{t=0}$$
$$=\mathrm{Tr}\left\{\frac{(\not{K}-m)}{4\omega_{\vec{k}}}[iS^>_{\vec{k}}(t,t)]_{t=0}\right\}.\quad (3.5)$$

We are considering the situation of $\mu\gg m$ so that we will neglect the current quark masses and consider the quarks as massless. Using the spectral representation of the propagators for Dirac fields given in the Appendix, we find, for massless fermions,

$$n_{\vec{k}}=\frac{1}{4}\int dq_0\ \mathrm{Tr}[\mathcal{P}_+(\vec{k})\rho_f(q_0,\vec{k})]N_f(q_0),\quad (3.6)$$

$$\overline{n}_{\vec{k}}=\frac{1}{4}\int dq_0\ \mathrm{Tr}[\mathcal{P}_-(\vec{k})\rho_f(q_0,\vec{k})][1-N_f(q_0)],\quad (3.7)$$

with $\mathcal{P}_\pm(\vec{k})$ given in the Appendix. Thus to obtain the quasi(anti)particle distribution functions we need to obtain the fermion spectral density $\rho(q_0,\vec{k})$.

The emission and absorption of hard gluons (photons) with momenta $q\gtrsim\mu$ will affect the distribution functions for fermions from deep within the Fermi sea up to excitations near the Fermi surface. However, because of the Pauli blocking of states below the Fermi surface, the emission and absorption of soft gluons (photons) with $q\ll\mu$ will only affect the distribution function of particles near the Fermi surface but not those deep within the Fermi sea. Soft gluons (photons) are sensitive to screening corrections and their propagator must include screening arising from quark loops. The leading order correction is given by the resummation of hard dense loops corresponding to quark intermediate states with momenta near the Fermi surface [34–37,33]. The spectral density in both cases, with hard and soft gluon exchange, will be studied in detail in the next section.

B. Equation of motion

We can treat the equilibrium and nonequilibrium aspects of cold and dense QED and QCD by studying the real-time equation of motion of a fermion condensate induced by an external source. The equilibrium aspects studied here can all be addressed by obtaining the fermion propagator and the fermionic spectral density, while the equation of motion allows us to study the real-time relaxation of an initially prepared condensate as an initial value problem prepared by using a suitable source term. The advantage of studying the equation of motion in real time is that it will reveal the relaxation of fermions directly in real time. Since the leading order corrections in the HDL approximation are similar for QED and QCD [34–37,33] and the gluon (photon) polarization is completely determined by the one fermion loop, we describe the necessary steps in QED; the final form for the spectral densities and relevant quantities for QCD can be obtained by simply accounting for the proper color and flavor factors.

The QED Lagrangian density in the Coulomb gauge is given by (see [38] for a similar context)

$$\mathcal{L}=\overline{\Psi}(i\not{\partial}-g\gamma^0A^0+g\vec{\gamma}\cdot\vec{A}_T)\Psi+\overline{\Psi}\eta+\overline{\eta}\Psi$$
$$+\tfrac{1}{2}[(\partial^\mu\vec{A}_T)^2+(\nabla A^0)^2],\quad (3.8)$$

where the Grassmann valued source terms were introduced to obtain the effective Dirac equation in the medium by analyzing the linear response to these sources.

Following the steps detailed in [38], we find the Dirac equation for the spatial Fourier transform of the expectation value in the massless case to be given by

$$\left(i\gamma_0 \frac{\partial}{\partial t} - \boldsymbol{\gamma}\cdot\vec{k} \right) \psi(\vec{k},t) + \int_{-\infty}^{\infty} dt' \;\; \Sigma(\vec{k},t-t') \;\; \psi(\vec{k},t') = -\eta(\vec{k},t), \tag{3.9}$$

where $\Sigma(\vec{k},t-t')$ is the retarded fermion self-energy given by the sum of the transverse and longitudinal contributions:

$$\Sigma(\vec{k},t-t') = \Sigma_T(\vec{k},t-t') + \Sigma_L(\vec{k},t-t'). \tag{3.10}$$

Using the results of the Appendix we find

$$\Sigma_T(\vec{k},t-t') = ig^2 \int \frac{d^3q}{(2\pi)^3} \mathcal{P}_{ij}(\mathbf{p}) (\gamma^i \{ [iS^{++}_{\vec{q}}(t,t')] \times [-i\mathcal{G}^{++}_{T,\vec{p}}(t,t')] - [iS^{<}_{\vec{q}}(t,t')] \times [-i\mathcal{G}^{<}_{T,\vec{p}}(t,t')] \} \gamma^j), \tag{3.11}$$

$$\Sigma_L(\vec{k},t-t') = ig^2 \int \frac{d^3q}{(2\pi)^3} (\gamma^0 \{ [iS^{++}_{\vec{q}}(t,t')] \times [-i\mathcal{G}^{++}_{L,\vec{p}}(t,t')] - [iS^{<}_{\vec{q}}(t,t')] \times [-i\mathcal{G}^{<}_{L,\vec{p}}(t,t')] \} \gamma^0), \tag{3.12}$$

with $\vec{p} = \vec{k} - \vec{q}$. The propagators are written in terms of their spectral representation and using the results in the Appendix it becomes clear that the retarded self-energy has the following causal structure:

$$\Sigma(\vec{k},t-t') = \Sigma^r(\vec{k},t-t')\Theta(t-t'). \tag{3.13}$$

Introducing the Fourier transforms in time for the expectation value of the Dirac field, the source and the self-energy, and the Fourier representation of $\Theta(t-t')$ we find that the equation of motion in terms of the space-time Fourier transforms becomes

$$[\gamma^0\omega - \vec{\gamma}\cdot\vec{k} + \tilde{\Sigma}(\omega,\vec{k})]\tilde{\psi}(\omega,\vec{k}) = -\tilde{\eta}(\omega,\vec{k}). \tag{3.14}$$

Introducing the dispersive representation for the retarded self-energy,

$$\tilde{\Sigma}(\omega,\vec{k}) = \frac{1}{\pi}\int dq_0 \, \frac{\mathrm{Im}\,\tilde{\Sigma}(q_0,\vec{k})}{q_0 - \omega - i0^+}, \tag{3.15}$$

a straightforward calculation reveals that

$$\Sigma^r(\vec{k},t-t') = \frac{1}{\pi}\int dq_0 \; e^{-iq_0(t-t')} \mathrm{Im}\,\tilde{\Sigma}(q_0,\vec{k}). \tag{3.16}$$

For massless fermions we write

$$\tilde{\Sigma}(\omega,\vec{k}) = \gamma^0\tilde{\Sigma}_0(\omega,\vec{k}) - \vec{\gamma}\cdot\hat{\vec{k}}\tilde{\Sigma}_1(\omega,\vec{k}). \tag{3.17}$$

Hence the solution of the equation of motion is given by

$$\tilde{\psi}(\omega,\vec{k}) = S_R(\omega,\vec{k})\,\tilde{\eta}(\omega,\vec{k}), \tag{3.18}$$

with

$$S_R(\omega,\vec{k}) = -\tfrac{1}{2}[\mathcal{P}_-(\vec{k})S_-(\omega,\vec{k}) + \mathcal{P}_+(\vec{k})S_+(\omega,\vec{k})], \tag{3.19}$$

$$S_-(\omega,\vec{k}) = [\omega - k + \tilde{\Sigma}_-(\omega,\vec{k})]^{-1}, \tag{3.20}$$

$$S_+(\omega,\vec{k}) = [\omega + k + \tilde{\Sigma}_+(\omega,\vec{k})]^{-1}, \tag{3.21}$$

$$\tilde{\Sigma}_-(\omega,\vec{k}) = \tilde{\Sigma}_0(\omega,\vec{k}) - \tilde{\Sigma}_1(\omega,\vec{k}), \tag{3.22}$$

$$\tilde{\Sigma}_+(\omega,\vec{k}) = \tilde{\Sigma}_0(\omega,\vec{k}) + \tilde{\Sigma}_1(\omega,\vec{k}), \tag{3.23}$$

with $\mathcal{P}_\pm(\vec{k})$ given in the Appendix. The fermion spectral density is obtained from the imaginary part of the retarded propagator and is given by

$$\rho_f(\omega,\vec{k}) = \tfrac{1}{2}[\mathcal{P}_-(\vec{k})\rho_-(\omega,\vec{k}) + \mathcal{P}_+(\vec{k})\rho_+(\omega,\vec{k})],$$

$$\rho_-(\omega,\vec{k}) = \frac{1}{\pi}\frac{\mathrm{Im}\,\tilde{\Sigma}_-(\omega,\vec{k})}{[\omega - k + \mathrm{Re}\,\tilde{\Sigma}_-(\omega,\vec{k})]^2 + [\mathrm{Im}\,\tilde{\Sigma}_-(\omega,\vec{k})]^2}, \tag{3.24}$$

$$\rho_+(\omega,\vec{k}) = \frac{1}{\pi}\frac{\mathrm{Im}\,\tilde{\Sigma}_+(\omega,\vec{k})}{[\omega + k + \mathrm{Re}\,\tilde{\Sigma}_+(\omega,\vec{k})]^2 + [\mathrm{Im}\,\tilde{\Sigma}_+(\omega,\vec{k})]^2}. \tag{3.25}$$

We consider two cases separately to obtain the spectral densities: (i) The gluon (photon) line in the fermion self-energy carries *hard* spatial momentum $p \geqslant \mu$. In this case one (bare) gluon exchange gives the leading order correction to the quark self-energy in the HDL approximation [34–37] for large chemical potential. (ii) The gluon (photon) line carries *soft* spatial momentum $p \ll \mu$ in which case the gluon (photon) propagator must be dressed by HDL fermion loops [34–37]. The contribution from hard gluon exchange to the self-energy of low momentum fermions deep within the Fermi sea, i.e., with $k \ll g\mu$, must be treated nonperturbatively [32,34–37], resulting in a modified dispersion relation and their description as quasiparticles. For fermions near the Fermi surface (and weak coupling) the HDL corrections from hard gluon exchange are perturbative. Thus hard gauge fields will modify the fermion propagators for all fermion states in the Fermi sea. On the other hand, the emission (and absorption) of soft gluons (photons) with $q \leqslant g\mu$ will only affect fermionic states *near the Fermi surface*. We now study each case in detail.

IV. EQUILIBRIUM ASPECTS

A. Hard gauge fields: Fermi liquid behavior

We are interested in particles near the Fermi surface; therefore we will focus on the spectral density $\rho_-(q_0,\vec{k})$ and we will neglect the antiparticles, for which there is no Fermi surface.

For hard gauge fields with loop momentum $q \gg \mu$ we can use the free field propagators for transverse and ''longitudinal'' gauge fields given in the Appendix. We find that the instantaneous Coulomb interaction leads to a local contribution to the self-energy which is subleading for small fermion momentum [36,37]. In the HDL limit we find

$$\rho_-(q_0,\vec{k}) = Z_+\,\delta(q_0-\omega_+(k)) + Z_-\,\delta(q_0+\omega_-(k)) + \rho_c(q_0,k), \tag{4.1}$$

with $\omega_+(k)$ and $\omega_-(k)$ the fermion and plasmino quasiparticle poles with residues $Z_\pm$, respectively (see [33] for their complete expressions). The continuum spectral density has support below the light cone and is given by

$$\rho_c(q_0,k) = \frac{1}{\pi}\,\frac{\mathrm{Im}\,\tilde{\Sigma}_-(\omega,\vec{k})}{[\omega-k+\mathrm{Re}\,\tilde{\Sigma}_-(\omega,\vec{k})]^2+[\mathrm{Im}\,\tilde{\Sigma}_-(\omega,\vec{k})]^2}, \tag{4.2}$$

$$\mathrm{Im}\,\tilde{\Sigma}_-(\omega,\vec{k}) = \pi\frac{M_f^2}{2k}\left(1-\frac{\omega}{k}\right)\Theta(k^2-\omega^2), \tag{4.3}$$

$$\mathrm{Re}\,\tilde{\Sigma}_-(\omega,\vec{k}) = -\frac{M_f^2}{2k}\left\{\left(1-\frac{\omega}{k}\right)\ln\left|\frac{\omega+k}{\omega-k}\right|+2\right\}, \tag{4.4}$$

$$M_f^2 = \frac{g^2\mu^2}{8\pi^2}, \tag{4.5}$$

and satisfies the sum rule

$$Z_+ + Z_- + \int_{-k}^{k} dq_0\,\rho_c(q_0,k) = 1. \tag{4.6}$$

The spectral densities $\rho_\pm(q_0,\vec{k})$ are related by [33]

$$\rho_+(q_0,\vec{k}) = \rho_-(-q_0,\vec{k}), \tag{4.7}$$

and upon using this relation, the results of the previous section, and the Appendix we find

$$n_{\vec{k}} = \int dq_0\,\rho_-(q_0,\vec{k})N(q_0), \tag{4.8}$$

$$\overline{n_{\vec{k}}} = \int dq_0\,\rho_-(q_0,\vec{k})\overline{N}(q_0), \tag{4.9}$$

$$N(q_0) = \Theta(\mu-q_0), \quad \overline{N}(q_0) = \Theta(-\mu-q_0), \tag{4.10}$$

and the fermion number density is given by

$$\mathcal{N} = \int \frac{d^3k}{(2\pi)^3}\int_{-\mu}^{\mu} dq_0\,\rho_-(q_0,\vec{k}). \tag{4.11}$$

This expression relates the chemical potential to the fermion number density. We now have the tools to understand the change in the Fermi sea in the HDL limit.

Since $N(q_0)=\Theta(\mu-q_0)$ and $\omega_+(k)>k$ [33], from the expression for the particle distribution function given by Eq. (4.8), we see that for values of k such that $\omega_+(k)<\mu$ the region of support of the spectral density $\rho_-(q_0,k)$ is contained in the interval $-\infty<q_0<\mu$; therefore for these values of k the distribution function is $n_k=1$. The value of the momentum at which the frequency of the fermion quasiparticle, $\omega_+(k)=\mu$, is the limiting value for which the quasiparticle pole is in the interval of support of $N(q_0)$, thus defining the Fermi momentum k_F by $\omega_+(k_F)=\mu$.

We can obtain an estimate for the value of the Fermi momentum in the HDL limit and weak coupling for which $\mu \gg M_f$ using the large k limit of the quasiparticle pole,

$$\omega_+(k) \approx k + \frac{M_f^2}{k}, \quad k \gg M_f, \tag{4.12}$$

from which we obtain

$$k_F \approx \mu\left[1-\frac{g^2}{8\pi^2}\right]. \tag{4.13}$$

For $k>k_F$ the quasiparticle pole is outside of the region of support of $N(q_0)$ but the spectral density still has a contribution inside this region, given by the plasmino pole at $-\omega_-(k)$ and the Landau damping continuum. Hence $n_{k>k_F}\neq 0$ as befits an interacting Fermi system. Thus, whereas for $k<k_F$ the distribution function $n_k=1$, for $k>k_F$ it is $0<n_{\vec{k}}<1$. This analysis leads to the following result:

$$n_{\vec{k}} = Z_-(k) + Z_+(k)\Theta(k_F-k) + \int_{-\mu}^{\mu}\rho_c(q_0,k) = \begin{cases} 1, & k=k_F-\epsilon, \\ 1-Z_+(k_F), & k=k_F+\epsilon. \end{cases} \tag{4.14}$$

We can estimate the discontinuity or ''jump'' at the Fermi surface in the HDL limit by using the sum rule (4.6) above and the large k limit of the quasiparticle residue [33]:

$$1-Z_+(k\approx k_F) \approx \left(\frac{g}{4\pi}\right)^2\left[2\ln\left(\frac{4\pi}{g}\right)-1\right]. \tag{4.15}$$

At the Fermi momentum we find

$$n_{k=k_F} = N(q_0=\mu)Z_+(k_F) + \left(\frac{g}{4\pi}\right)^2\left[2\ln\left(\frac{4\pi}{g}\right)-1\right], \tag{4.16}$$

where we have used $N(q_0=\mu)=1/2$. Thus, to this order, the Fermi surface is sharp with a jump discontinuity at $k=k_F$ given by $n_{k=k_F-\epsilon}-n_{k=k_F+\epsilon}=Z_+(k_F)$. The sharpness of the

Fermi surface in the HDL approximation is a consequence that to this order the quasiparticle excitations have an infinite lifetime. For momenta $k\approx\mu$ the HDL approximation is not truly justified since in this limit $k\gg g\mu$ and the contribution from the hard momentum region of the two particle cut is of $\mathcal{O}(g^2\mu)$ which becomes comparable to that of Landau damping of $\mathcal{O}(g^2\mu^2/k)$. This fact notwithstanding, the main purpose of this analysis is to reveal that the contribution from the hard loop momentum region to lowest order in the resummation program leads to a description consistent with Fermi liquid theory with a discontinuity or ''jump'' at the Fermi surface determined by the residue of the quasiparticle pole which to this order is non-vanishing. As we will study in detail below, the contribution from soft gluon exchange, which requires screening corrections, invalidates the Fermi liquid description.

B. Soft gauge fields: Non Fermi liquid

We now focus on the damping effects on quasiparticles near the Fermi surface, i.e., $k\approx k_F\approx\mu$. Damping of these excitations results from the emission and absorption of soft gluons which require the gluon (photon) propagators in the fermion self-energy to be HDL resummed [32–37]. These dressed gauge propagators can be handily included in the calculation of the self-energy by writing the Wightman functions for the gauge fields in terms of their spectral representation described in the Appendix. Since the fermion momentum is $k\approx k_F\approx\mu$ and the exchanged gluon is soft with $q\ll\mu$, the fermion line in the self-energy does not require HDL resummation and can be taken to be a bare fermion propagator.

A straightforward calculation using the free fermion propagators for the internal fermion line and the HDL resummed longitudinal and transverse gauge field propagators in terms of their spectral densities leads to the fermion self-energy in a dispersive representation as in Eq. (3.15) with

$$\begin{aligned}\mathrm{Im}\,\widetilde{\Sigma}(q_0,\vec{k}) = \frac{\pi g^2}{2}\int\frac{d^3q}{(2\pi)^3}\int dp_0\{&[\Theta(p_0)-\Theta(\mu-q)]\\ &\times\delta(q_0-p_0-q)[\widetilde{\rho}_T(p_0,p)\mathcal{P}_T^{ij}(\mathbf{p})\gamma^i\mathcal{P}_-(\mathbf{q})\gamma^j\\ &+\widetilde{\rho}_L(p_0,p)\gamma^0\mathcal{P}_-(\mathbf{q})\gamma^0]\\ &+\Theta(p_0)\delta(q_0+p_0+q)\\ &\times[\widetilde{\rho}_L(p_0,p)\mathcal{P}_T^{ij}(\mathbf{p})\gamma^i\mathcal{P}_+(\mathbf{q})\gamma^j\\ &+\widetilde{\rho}_L(p_0,p)\gamma^0\mathcal{P}_+(\mathbf{q})\gamma^0]\},\end{aligned}\tag{4.17}$$

where $\vec{p}=\vec{k}-\vec{q}$ and we have neglected the instantaneous Coulomb interaction. $\widetilde{\rho}_{T,L}$ are given in the Appendix.

The dispersive representation (3.15) makes clear that the largest contribution to the self-energy for $\omega\approx\mu$ is determined by the behavior of $\mathrm{Im}\,\Sigma(q_0,k)$ for $q_0\approx\omega\approx\mu$.

The contribution from soft gluons to the self-energy of fermions near the Fermi surface $k\approx\mu$ can be extracted easily by first relabelling the integration momenta $\vec{p}\leftrightarrow\vec{k}-\vec{q}$ so that $\vec{q}$ is the momentum of the (soft) gluon line with $q\ll\mu$ and $|\vec{k}-\vec{q}|\approx k-q\cos(\theta)$ with θ the angle between $\vec{k}$ and $\vec{q}$. In this limit we find

$$\begin{aligned}\mathrm{Im}\,\widetilde{\Sigma}_-(q_0,k) = \pi g^2\int\frac{d^3q}{(2\pi)^3}\int dp_0(\{&\rho_T(p_0,q)\\ &\times[1-\cos^2(\theta)]+\rho_L(p_0,q)\}\\ &\times[\Theta(p_0)-\Theta(\mu-k+q\cos(\theta))]\\ &\times\delta(q_0-p_0-k+q\cos(\theta))+\rho_T(p_0,q)\\ &\times[1+\cos^2(\theta)]\Theta(p_0)\delta(q_0+p_0\\ &+k-q\cos(\theta))),\end{aligned}\tag{4.18}$$

$$\begin{aligned}\mathrm{Im}\,\widetilde{\Sigma}_+(q_0,k) = \pi g^2\int\frac{d^3q}{(2\pi)^3}\int dp_0(\rho_T(p_0,q)&\\ &\times[1+\cos^2(\theta)]\\ &\times[\Theta(p_0)-\Theta(\mu-k+q\cos(\theta))]\\ &\times\delta(q_0-p_0-k+q\cos(\theta))+\{\rho_T(p_0,q)\\ &\times[1-\cos^2(\theta)]+\rho_L(p_0,q)\}\Theta(p_0)\\ &\times\delta(q_0+p_0+k-q\cos(\theta))).\end{aligned}\tag{4.19}$$

For particles near the Fermi surface the quark propagator has poles near $\omega\approx k\approx\mu$, while for antiparticles there is no Fermi surface and the poles are at $\omega\approx-k$. Therefore for particles the self-energy is determined by $\mathrm{Im}\,\widetilde{\Sigma}_+(q_0,k)$ for $q_0\approx\omega$ through the dispersion relation. Hence for particles near the Fermi surface the important region is $q_0\approx\omega\approx k$ which implies that the argument of $\delta(q_0-p_0-k+q\cos(\theta))$ has support for $p_0\approx q\cos(\theta)$ corresponding to the region of Landau damping of the gluon (photon) propagator (see the Appendix). On the other hand, for $q_0\approx k\approx\omega\approx\mu$ the $\delta(q_0+p_0+k-q\cos(\theta))$ has support in the region of $p_0\approx-2\mu<0$ and this contribution is canceled by the $\Theta(p_0)$. Thus the contribution to the self-energy of particles near the Fermi momentum from soft gluon exchange is completely determined by the first delta function

$$\begin{aligned}\mathrm{Im}\,\widetilde{\Sigma}_-(q_0,k)\approx\pi g^2\int\frac{d^3q}{(2\pi)^3}(\{&\rho_T(p_0,q)[1-\cos^2(\theta)]\\ &+\rho_L(p_0,q)\}[\Theta(q_0-k+q\cos(\theta))\\ &-\Theta(\mu-k+q\cos(\theta))])_{p_0=q_0-k+q\cos\theta},\end{aligned}\tag{4.20}$$

which obviously vanishes at $q_0=\mu$. Thus we see that the imaginary part of the self-energy i.e., the damping rate for fermionic excitations, vanishes at the Fermi surface [36,37]. For antiparticles the propagator has poles for $\omega\approx-k$, and for hard momentum $k\approx\mu$ and $q_0\approx-k$ the $\delta(q_0-p_0-k+q\cos(\theta))$ has support for $p_0\approx-2k\approx-2\mu$, i.e, in the hard region, while $\delta(q_0+p_0+k-q\cos(\theta))$ has support for $p_0=$

$-q_0-k+q\cos(\theta)\approx q\cos(\theta)$ which is in the Landau damping region of the spectral density. Hence

$$\mathrm{Im}\,\tilde{\Sigma}_+(q_0,k)\approx \pi g^2\int\frac{d^3q}{(2\pi)^3}(\{\rho_T(p_0,q)[1-\cos^2(\theta)] + \rho_L(p_0,q)\}\Theta(p_0))_{p_0=-q_0-k+q\cos(\theta)}. \tag{4.21}$$

The case of antiparticles has been studied in [37,35] with the result that the self-energy is analytic near the Fermi surface and does not lead to novel phenomena. Hence in what follows we will ignore the case of antiparticles and refer the reader to [37,35] for more details on this case.

Since the imaginary part of the self-energy for particles vanishes at the Fermi surface, we expand near $q_0\approx\mu$ as follows:

$$\Theta(q_0-k+q\cos(\theta))-\Theta(\mu-k+q\cos(\theta)) = \tilde{q}_0\,\delta(q\cos(\theta)-(k-\mu))+\cdots, \tag{4.22}$$

with

$$\tilde{q}_0=(q_0-\mu), \tag{4.23}$$

and we are led to the expression

$$\mathrm{Im}\,\tilde{\Sigma}_-(q_0,k)\approx\frac{g^2}{4\pi}\tilde{q}_0\int_{|k-\mu|}^{q^*}\left[\rho_T(\tilde{q}_0,q)\times\left(1-\frac{(k-\mu)^2}{q^2}\right)+\rho_L(\tilde{q}_0,q)\right]dq. \tag{4.24}$$

For $\tilde{q}_0\to 0$ we can approximate:

$$\rho_T(\tilde{q}_0,q)\approx\frac{M^2\left(\frac{\tilde{q}_0}{q}\right)\Theta(q^2-\tilde{q}_0^2)}{\left[q^2+4M^2\left(\frac{\tilde{q}_0^2}{q^2}\right)\right]^2+\left[\frac{\pi M^2\tilde{q}_0}{q}\right]^2}, \tag{4.25}$$

$$\rho_L(\tilde{q}_0,q)\approx\frac{2M^2\left(\frac{\tilde{q}_0}{q}\right)}{[q^2+4M^2]^2}\Theta(q^2-\tilde{q}_0^2), \tag{4.26}$$

$$M^2=\frac{g^2\mu^2}{4\pi^2}. \tag{4.27}$$

The region in which dynamical screening via Landau damping is effective is determined by $q,|\tilde{q}_0|<M$; hence the validity of the approximation invoked above relies on $|\tilde{q}_0|<M$.

We note that whereas ρ_T has a strong infrared singularity for $q\to 0$ when $\tilde{q}_0\to 0$, Debye screening cuts off the infrared behavior of ρ_L which leads to the conclusion that the contribution from the longitudinal gluons (photons) is $\propto\tilde{q}_0^2$ [37]. For excitations at the Fermi surface with $k=\mu$ the contribution to the imaginary part from the transverse photons can be computed straighforwardly and it yields

$$\mathrm{Im}\,\tilde{\Sigma}_-^{(a)}(q_0,k)=\frac{g^2}{24\pi}|\tilde{q}_0|. \tag{4.28}$$

The contribution from the longitudinal gluons (photons) is clearly of $\mathcal{O}(g^2\tilde{q}_0^2)$ and of the same order as the contribution from the hard gluon (photon) region [37]. This is similar to the case of nonrelativistic electrons interacting via the screened Coulomb interaction [43]. The term proportional to $\tilde{k}=k-\mu$ in Eq. (4.24) can be easily shown to yield a contribution of $\mathcal{O}(g^2(\tilde{k}^2/M)|\tilde{\omega}/M|^{1/3})$.

Therefore we conclude that

$$\mathrm{Im}\,\tilde{\Sigma}_-(q_0,k)=\frac{g^2}{24\pi}|\tilde{q}_0|+Ag^2\frac{\tilde{q}_0^2}{M}+B\left(g^2\frac{\tilde{k}^2}{M}\left|\frac{\tilde{\omega}}{M}\right|^{1/3}\right), \tag{4.29}$$

with calculable coefficients A,B. This result was previously obtained in Refs. [35,36]. Our focus is to understand the quasiparticle excitations and their distribution function very near the Fermi surface, in particular the discontinuity of the distribution function at k_F. In order to do this we need only consider $\tilde{k}\ll M$ with $|\tilde{\omega}|\ll M$; therefore we will keep only the first (leading) contribution in Eq. (4.29).

We can now obtain the self-energy via the dispersion relation (3.15) for $\omega\approx\mu$ by using the first term of Eq. (4.29) and integrating within a region of width $\approx M$ around μ since this is the region in which Landau damping is effective for dynamical screening and the region that yields the leading infrared contribution.

We finally obtain, for $k,q_0\approx\mu$,

$$\tilde{\Sigma}_-(\omega,k=\mu)=-\frac{g^2}{24\pi^2}\tilde{\omega}\left\{\ln\left[-\frac{\tilde{\omega}+i0^+}{M}\right]+\ln\left[\frac{\tilde{\omega}+i0^+}{M}\right]\right\} = -\frac{g^2}{12\pi^2}\tilde{\omega}\ln\left|\frac{\tilde{\omega}}{M}\right|+i\frac{g^2}{24\pi}|\tilde{\omega}|, \tag{4.30}$$

$$\tilde{\omega}=\omega-\mu, \tag{4.31}$$

which combines the results of Refs. [17,36] into the real and imaginary parts of the quark self-energy near the Fermi surface. We finally obtain the retarded propagator and spectral densities for particles near the Fermi surface by using the relations (3.19)–(3.25) and extracting the term proportional to $\mathcal{P}_-(\vec{k})$.

It is convenient to introduce $\tilde{k}=k-\mu\approx k-k_F$ (since from the analysis of the previous section $k_F=\mu[1-\mathcal{O}(g^2)]$); for $\omega,k\approx\mu$ the inverse propagators for particles can be written as

$$S_-^{-1}(\omega,k)\approx\tilde{\omega}-\tilde{k}+\tilde{\Sigma}_-(\omega,k=\mu). \tag{4.32}$$

The form of the real part of the self-energy $\propto \tilde{\omega}\ln|\tilde{\omega}/M|$ strongly suggests a wave function renormalization. Such an interpretation is obscured by the term $\tilde{k}$ in the propagator; however, *at the Fermi surface* with $\tilde{k}=0$, the logarithmic singularities of infrared origin are reminiscent of those of a *critical theory* and the propagator is similar to that obtained in perturbation theory in a critical theory at the upper critical dimensionality. This interpretation is validated by the current ideas on Fermi liquid theory based on the renormalization group, which describes the effective theory near the Fermi surface as a critical theory with marginal Fermi liquid interactions [44].

Since at the Fermi surface ($\tilde{k}=0$) the inverse propagator is proportional to $\tilde{\omega}$, the wave function renormalization constant at the (quasi)particle pole for excitations near the Fermi surface would be given by

$$Z(\mu)=\left[1+\frac{d}{d\omega}\mathrm{Re}\,\tilde{\Sigma}_{-}(\omega,k)\big|_{\omega=k=\mu}\right]^{-1}$$

$$\approx\frac{1}{\left[1-\dfrac{g^2}{12\pi^2}\ln\left|\dfrac{\tilde{\omega}}{\mu}\right|\right]}\tilde{}_{\omega=0}. \tag{4.33}$$

This wave function renormalization or residue at the (quasi)particle pole for excitations near the Fermi surface is precisely the quantity that determines the ''jump'' of the (quasi)particle distribution function at the Fermi surface as determined by Eq. (4.16). However, the logarithmic singularities manifest in Eq. (4.30) would lead to the conclusion that $Z(\mu)=0$ and that the Fermi surface ''vanishes.'' Such conclusion has also been obtained in nonrelativistic systems with magnetic interactions [28–30].

A similar situation arises in a critical theory; for example, in the Euclidean formulation of a critical scalar theory with quartic interaction in four dimensions the inverse propagator for small Euclidean four-momentum K is given by

$$G^{-1}(K)\approx K^2[1-\lambda^2 c\ln(K^2/\kappa^2)], \tag{4.34}$$

with λ the quartic coupling, c a combinatoric constant, and κ a renormalization scale. Again the wave function renormalization or residue at the ''pole'' $K^2=0$,

$$Z=\left[\frac{d}{dK^2}G^{-1}(K)\bigg|_{K^2=0}\right]^{-1}, \tag{4.35}$$

vanishes. The vanishing of the wave function renormalization on the particle mass shell in a critical theory indicates that the propagator acquires an *anomalous* scaling dimension. The logarithmic singularities are resummed via the renormalization group, leading to the following improved propagator:

$$G^{-1}_{RG}(K)=K^2\left(\frac{K^2}{\kappa^2}\right)^{-\eta},\quad \eta=\lambda^2 c. \tag{4.36}$$

Therefore we interpret the vanishing of the wave function renormalization for quasiparticles at the Fermi surface as an indication of the buildup of an anomalous dimension as a consequence of the infrared singularities, which are only dynamically screened via Landau damping. To make this interpretation explicit we now proceed to obtain a renormalization group improved quasiparticle propagator, focusing solely on the particle excitations near the Fermi surface.

C. Euclidean renormalization group

1. $\tilde{k}=0$

In order to obtain a renormalization group resummation of the infrared singularities we must first perform an analytical continuation to Euclidean space. This is accomplished by the following analytical continuation:

$$\tilde{\omega}+i0^{+}=iK, \tag{4.37}$$

with K taken to be a real variable. From Eq. (3.20) the particle propagator now reads

$$S_{-}(\omega,k)\big|_{\omega\approx 0,k=0}=-i\frac{K}{\Gamma(K)}, \tag{4.38}$$

$$\Gamma(K)=K^2\left[1-\lambda\ln\left(\frac{K^2}{M^2}\right)\right],$$

$$\lambda=\frac{g^2}{24\pi^2}. \tag{4.39}$$

Obviously $\Gamma(K)$ has the same form as the inverse propagator of a scalar theory with infrared corrections typical of a critical theory as discussed above. The physics near the Fermi surface requires $K\ll M$, which obviously leads to a breakdown of the perturbative expansion. Just as in a critical theory taking $K\to 0$ and keeping M fixed is the same as keeping K fixed and taking $M\to\infty$, i.e, interpreting M as an ultraviolet cutoff and taking the limit of large cutoff at a fixed transferred momentum.

The renormalization group improvement proceeds in the same manner as in the scalar theory; we first introduce a wave function renormalization constant that will absorb the cutoff dependence at a given renormalization scale κ and a renormalized vertex function

$$\Gamma_R(K,\kappa)=Z[\kappa,M]\Gamma(K,M), \tag{4.40}$$

$$Z[\kappa]=1+\lambda\ln\left[\frac{\kappa^2}{M^2}\right]+\cdots. \tag{4.41}$$

The independence of the bare vertex upon the renormalization scale leads to the renormalization group equation

$$\left[\kappa\frac{\partial}{\partial\kappa}-\eta\right]\Gamma_R(K,\kappa)=0, \tag{4.42}$$

$$\eta=\frac{\kappa}{Z}\frac{\partial Z}{\partial\kappa}=2\lambda. \tag{4.43}$$

Using the fact that the vertex has scaling dimension 2, i.e.,

$$\Gamma_R(K,\kappa)=\kappa^2\Phi\left(\frac{K}{\kappa}\right), \tag{4.44}$$

with Φ a dimensionless function of its argument, the renormalization group equation for the scaling function Φ can be solved straightforwardly, leading to

$$\Gamma_R(K,\kappa)=\kappa^2\left[\frac{K}{\kappa}\right]^{2-\eta}\Phi(1). \tag{4.45}$$

We can now obtain a renormalization group improved vertex function as follows. Requiring that at the scale $K=M$ (i.e., at the scale of the cutoff where perturbation theory is valid) the ''bare'' vertex obey

$$\Gamma(K=M,M)=M^2=Z^{-1}[\kappa,M]\Gamma_R[K=M,\kappa] \tag{4.46}$$

fixes the *renormalization group resummed* wave function renormalization in terms of the solution of the renormalization group equation (4.45) at the scale $K=M$. The renormalization group improved ''bare vertex'' $\Gamma(K,M)=Z^{-1}[\kappa,M]\Gamma_R[K,\kappa]$ is valid for $K\ll M$ and leads to the following resummed particle propagator valid for $k=k_F$, $\tilde{\omega}<M$ and weak coupling $\lambda\ll 1$:

$$S_-(\omega,k)|_{\tilde{\omega}\approx 0,\tilde{k}=0}=-\frac{i}{M}\left[\frac{K^2}{M^2}\right]^{\lambda-1/2}. \tag{4.47}$$

The resummed spectral density for particles $\rho_-(\omega,k)=\mathrm{Im}\,S_-(\omega,k)/\pi$ is obtained by performing the analytic continuation $K\to -i\tilde{\omega}+0^+$, leading to the following expression near the Fermi surface:

$$\rho_-(\omega,k)|_{\omega\approx\mu,k=\mu}=\frac{\sin[\pi\lambda]}{\pi|\tilde{\omega}|}\left|\frac{\tilde{\omega}}{M}\right|^{2\lambda},\quad \tilde{\omega}=\omega-\mu,$$

$$\lambda=\frac{g^2}{24\pi^2}. \tag{4.48}$$

It is straightforward to check that this spectral density becomes a delta function in the limit $\lambda\to 0$ by integrating it within a small region around the Fermi surface. This spectral density is remarkably similar to that found in non-Fermi-liquid systems such as Luttinger liquids and has been experimentally measured in condensed matter systems via the x-ray edge singularities at the Fermi surface of some metals [42].

Using the renormalization group improved spectral density (4.48) we can now obtain the value of the particle distribution function at the Fermi surface by restricting the integral in Eq. (4.8) to a region of width M near the Fermi surface:

$$n_{\vec{k}=\vec{k}_F}=\int_{-M}^{M}d\tilde{\omega}\;\;\Theta(-\tilde{\omega})\frac{\sin[\pi\lambda]}{\pi\tilde{\omega}}\left|\frac{\tilde{\omega}}{M}\right|^{2\lambda}=N_{\vec{k}=\vec{k}_F}\frac{\sin[\pi\lambda]}{\pi\lambda}, \tag{4.49}$$

with $N_{\vec{k}}$ the Fermi-Dirac distribution function and $N_{\vec{k}=\vec{k}_F}=1/2$. The distribution function (4.49) obviously attains the free field limit for $\lambda\to 0$.

2. $\tilde{k}\neq 0$

The renormalization group method presented above for the case of $\tilde{k}=0$ can be straightforwardly extended to $\tilde{k}\neq 0$ by recognizing that the propagator for $\tilde{k}\neq 0$ is

$$\Gamma(K)=K^2\left[1-\lambda\ln\left(\frac{K^2}{M^2}\right)\right]+iK\tilde{k}, \tag{4.50}$$

similar to that obtained in a scalar theory in the large transferred momentum limit but with a ''mass'' term. This similarity suggests that the term $i\tilde{k}K$ can be treated just as a mass term in the renormalization program of a scalar theory. Therefore, along with the wave function renormalization (4.40) we also introduce the multiplicative renormalization

$$\tilde{k}_R=Z[\kappa,M]\tilde{k}. \tag{4.51}$$

Since there are no infrared divergences associated with $\tilde{k}$, then $Z[\kappa,M]$ is chosen in perturbation theory to be that of the $\tilde{k}=0$ case discussed above and is independent of $\tilde{k}$.

The renormalization group equation now becomes

$$\left[\kappa\frac{\partial}{\partial\kappa}-\eta+\gamma\tilde{k}_R\frac{\partial}{\partial\tilde{k}_R}\right]\Gamma_R(K,\tilde{k}_R,\kappa)=0, \tag{4.52}$$

$$\eta=\frac{\kappa}{Z}\frac{\partial Z}{\partial\kappa}=2\lambda, \tag{4.53}$$

$$\gamma=\frac{\kappa}{\tilde{k}_R}\frac{\partial\tilde{k}_R}{\partial\kappa}=2\lambda. \tag{4.54}$$

Using the fact that the vertex function has dimension 2, we write

$$\Gamma_R(K,\tilde{k}_R,\kappa)=\kappa^2\Phi\left(\frac{K}{\kappa};\frac{\tilde{k}_R}{\kappa}\right). \tag{4.55}$$

Finally introducing the variables and *Ansätze*

$$\frac{K}{\kappa}=e^{-t},\quad r=\frac{\tilde{k}_R}{\kappa}, \tag{4.56}$$

$$\Phi(e^{-t},r)=e^{t(\eta-2)}H[t,r], \tag{4.57}$$

the function $H[t,r]$ obeys the simple renormalization group equation

$$\left[\frac{\partial}{\partial t}+\overline{\gamma} r\frac{\partial}{\partial r}\right]H[t,r]=0, \tag{4.58}$$

$$\overline{\gamma}=\gamma-1=2\lambda-1. \tag{4.59}$$

The solution of this equation is simple,

$$H[t,r]=H[\overline{r}(t)], \tag{4.60}$$

with $\overline{r}(t)$ the solution of the ordinary differential equation

$$\frac{d\overline{r}}{dt}=-\overline{\gamma r}\Rightarrow\overline{r}(t)=\overline{r}(0)e^{-\overline{\gamma}t}. \tag{4.61}$$

Therefore we find that the renormalization group improved vertex function is given by

$$\Gamma_R(K,\tilde{k},\kappa)=K^2\left(\frac{K^2}{\kappa^2}\right)^{-\lambda}H\left[\frac{\tilde{k}\mathcal{Z}}{K}\left(\frac{K^2}{\kappa^2}\right)^{\lambda}\right], \tag{4.62}$$

where we have explicitly used the multiplicative renormalization of $\tilde{k}$ and introduced the integration constant $\mathcal{Z}$, which only depends on κ and M, to be determined later.

Comparison with the solution (4.45) for $\tilde{k}=0$ reveals that $H[0]=\Phi(1)$. As in the case $\tilde{k}=0$ we request that the ''bare'' vertex coincide with the free field expression at the cutoff scale $K=M$, i.e.,

$$\Gamma[M,\tilde{k},M]=M^2\left[1+i\frac{\tilde{k}}{M}\right]=Z^{-1}[\kappa,M]\Gamma_R[M,\tilde{k},\kappa]. \tag{4.63}$$

This condition and the identification $H[0]=\Phi(1)$ determine *both* $Z[\kappa,M]$ and $\mathcal{Z}[\kappa,M]$ by comparing the powers of $\tilde{k}$. Since H is a function of the *scaling variable* $\varphi=\tilde{k}\mathcal{Z}(K/\kappa)^{2\lambda}$, the functional form of $H[\varphi]$ is uniquely determined for $\tilde{k}\ll M$. We are thus led to the following unique form of the renormalization group resummed vertex function for $\tilde{k}\ll M$, $\lambda\ll 1$:

$$\Gamma(K,\tilde{k})=K^2\left(\frac{K^2}{M^2}\right)^{-\lambda}\left[1+\frac{i\tilde{k}K}{K^2\left(\frac{K^2}{M^2}\right)^{-\lambda}}\right]. \tag{4.64}$$

This discussion reveals another manifestation of the critical nature of the theory near the Fermi surface: the renormalization group improved vertex function is of the *scaling form*

$$\Gamma(K,\tilde{k})=\Gamma(K,0)D\left[\frac{\tilde{k}}{K^{\Delta}}\right],\quad \Delta=1-2\lambda. \tag{4.65}$$

Using the relation between the vertex function and the Euclidean particle propagator given by Eq. (4.38) we find, from Eq. (4.64),

$$S_-(\omega,k)_{\omega\approx\mu,k\approx\mu}=\frac{1}{\left[iK\left(\frac{K}{M}\right)^{-2\lambda}-\tilde{k}\right]},\quad K=-i\tilde{\omega}+0^+. \tag{4.66}$$

We can now obtain the spectral density near the Fermi surface by following the steps detailed in the case $\tilde{k}=0$, leading to

$$\rho_-(\omega,k)\big|_{\omega\approx\mu,k\approx\mu}=\frac{\sin[\pi\lambda]}{\pi}|\tilde{\omega}|\left|\frac{\tilde{\omega}}{M}\right|^{-2\lambda}\frac{1}{\left[\left(\tilde{\omega}\left|\frac{\tilde{\omega}}{M}\right|^{-2\lambda}-\tilde{k}\cos[\pi\lambda]\right)^2+(\tilde{k}\sin[\pi\lambda])^2\right]}, \tag{4.67}$$

which vanishes identically at $\tilde{\omega}=0$. This spectral density is displayed as a function of $\tilde{\omega}$ for several values of $\tilde{k}$ and λ in Figs. 1 and 2.

3. Quasiparticles

Figures 1 and 2 clearly reveal that in weak coupling the spectral density features a narrow resonance for $\tilde{k}\neq 0$, the position of which is obtained by the vanishing of the first term in the denominator in Eq. (4.67) which determines the *quasiparticle dispersion relation*. It is given by

$$\tilde{\omega}_p(\tilde{k})=\mathrm{sgn}(\tilde{k})[|\tilde{k}|M^{-2\lambda}\cos(\pi\lambda)]^{1/(1-2\lambda)}. \tag{4.68}$$

We note that the group velocity of the quasiparticles near the Fermi surface,

$$v_g(\tilde{k})=[M^{-2\lambda}\cos[\pi\lambda]]^{1/(1-2\lambda)}\frac{|\tilde{k}|^{2\lambda/(1-2\lambda)}}{(1-2\lambda)}, \tag{4.69}$$

vanishes as $k\to k_F$. We interpret this novel phenomenon in terms of a collective backflow that surrounds the quasiparticle.

Near the position of the resonance, i.e., for $\tilde{\omega}\approx\tilde{\omega}_p$, the spectral density can be approximated by a Breit-Wigner form

$$\rho_-(\omega,k)\big|_{\tilde{\omega}\approx\tilde{\omega}_p,k\approx\mu}=Z_p[\tilde{k}]\frac{\cos[\pi\lambda]}{\pi}\frac{\Gamma(\tilde{k})}{[\tilde{\omega}-\tilde{\omega}_p(\tilde{k})]^2+\Gamma^2(\tilde{k})}, \tag{4.70}$$

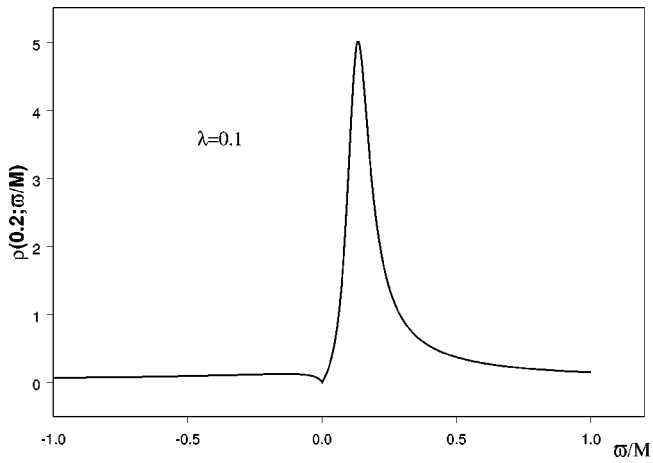

FIG. 1. $\rho_-(\tilde{k}/M,\tilde{\omega}/M)$ for $\lambda=0.1$, $\tilde{k}/M=0.2$.

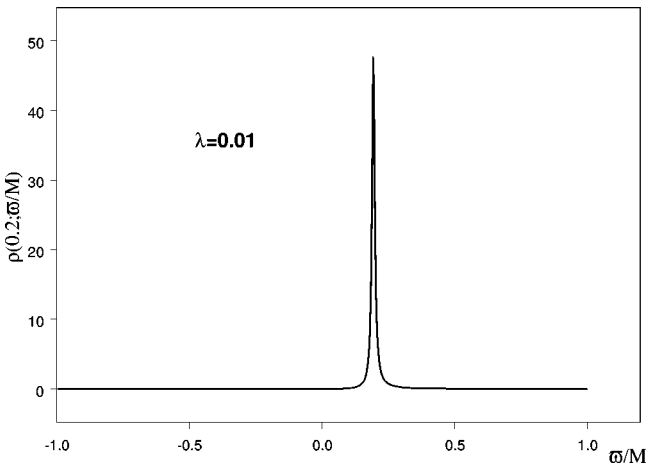

FIG. 2. $\rho_-(\tilde{k}/M,\tilde{\omega}/M)$ for $\lambda=0.01$, $\tilde{k}/M=0.2$.

$$Z_p[\tilde{k}]=\frac{\left|\dfrac{\tilde{\omega}_p(\tilde{k})}{M}\right|^{2\lambda}}{(1-2\lambda)}, \tag{4.71}$$

$$\Gamma(\tilde{k})=Z_p[\tilde{k}]|\tilde{k}|\sin[\pi\lambda]. \tag{4.72}$$

Therefore the residue of the ''quasiparticle pole'' and the ''quasiparticle width'' vanishes near the Fermi surface as

$$Z_p[\tilde{k}]\propto|k-k_F|^{2\lambda/(1-2\lambda)}, \tag{4.73}$$

$$\Gamma(\tilde{k})\propto|k-k_F|^{1/(1-2\lambda)}. \tag{4.74}$$

It is straightforward to confirm that the quark propagator (4.66) has a complex pole with the real and imaginary parts given by Eqs. (4.68) and (4.72), respectively, in the narrow width approximation $\Gamma(\tilde{k})/\tilde{\omega}_p(\tilde{k})\ll 1$. For this purpose write, for the complex pole,

$$K_p=-i\tilde{\omega}_p-\Gamma, \tag{4.75}$$

with $\Gamma>0$ corresponding to damping (this is confirmed *a posteriori* from the solution). In the narrow width approximation we can replace

$$(\tilde{\omega}_p-i\Gamma)^{1-2\lambda}\approx(\tilde{\omega}_p)^{1-2\lambda}\left[1-(1-2\lambda)i\ \frac{\Gamma}{\tilde{\omega}_p}+\cdots\right]. \tag{4.76}$$

Requiring the vanishing of the real and imaginary parts of the denominator of Eq. (4.66) we find the position of the quasiparticle pole and its width given by Eqs. (4.68) and (4.72), respectively.

4. Requiem to the Fermi liquid: The jump of the distribution function at k_F vanishes

We can now study the behavior of the distribution function near the Fermi surface by using the spectral density (4.67) in the expression (4.8). Since the domain of validity of the approximations invoked to obtain the spectral density is such that $|\tilde{\omega}|$, $|\tilde{k}|<M$, the integral in the variable $\tilde{\omega}$ must be cut off at the scale M. Hence we find

$$n_{\vec{k}}=n_{\vec{k}_F}+\Delta n(\tilde{k}), \tag{4.77}$$

$$n_{\vec{k}_F}=\frac{\sin[\pi\lambda]}{2\pi\lambda}, \tag{4.78}$$

$$\Delta n(\tilde{k})=\int_{-M}^{0}d\tilde{\omega}[\rho_-(\tilde{\omega},\tilde{k})-\rho_-(\tilde{\omega},0)]. \tag{4.79}$$

A detailed calculation reveals that

$$\begin{aligned}\Delta n(\tilde{k})&=-\frac{\tilde{k}}{\pi M}\sum_{n=0}^{\infty}\frac{(-\tilde{k}/M)^n\ \sin[(n+2)\pi\lambda]}{n+1-2(n+2)\lambda}\\&=-\frac{\tilde{k}}{\pi M}\left[\frac{\sin 2\pi\lambda}{1-4\lambda}-\frac{\tilde{k}\ \sin 3\pi\lambda}{M(2-6\lambda)}+\frac{\tilde{k}^2\ \sin 4\pi\lambda}{M^2(3-8\lambda)}\right.\\&\quad\left.+\mathcal{O}(\tilde{k}^3)\right],\end{aligned} \tag{4.80}$$

leading to the following form of the single quasiparticle distribution near the Fermi momentum:

$$n_{\vec{k}\approx\vec{k}_F}=\frac{\sin[\pi\lambda]}{2\pi\lambda}-\frac{\tilde{k}}{\pi M(1-4\lambda)}+\mathcal{O}(\tilde{k}^2). \tag{4.81}$$

As was originally pointed out in Refs. [14,17] the exchange of dynamically screened magnetic gluons leads to the breakdown of the Fermi liquid description. The renormalization group resummation of the infrared divergences responsible for the breakdown of the Fermi liquid picture leads to Eq. (4.81) and therefore to the vanishing of the discontinuity of the distribution function at the Fermi surface. This is one of the important results of this work.

This is clearly a consequence of the result that the wave function renormalization or residue at the quasiparticle pole vanishes as a power law at the Fermi surface. In Fermi liquid

theory, the discontinuity at the Fermi surface enters in all thermodynamic response functions, for example, in the coefficient of the linear power of temperature in the specific heat [41,42]; thus the vanishing of the jump discontinuity will likely result in an anomalous specific heat.

V. NONEQUILIBRIUM ASPECTS: SINGLE QUASIPARTICLE RELAXATION

A. Dynamical renormalization group

The equation of motion (3.9) can be written in the form

$$\left(i\gamma_0 \frac{\partial}{\partial t} - \boldsymbol{\gamma}\cdot\vec{k} \right) \psi(\vec{k},t) + \int_{-\infty}^{t} dt' \;\; \Sigma^r(\vec{k},t-t') \;\; \psi(\vec{k},t') = -\eta(\vec{k},t), \tag{5.1}$$

with

$$\Sigma^r(\vec{k},t-t') = \frac{i}{\pi}\int d\omega \, \mathrm{Im}\,\widetilde{\Sigma}(\omega,\vec{k}) e^{-i\omega(t-t')}. \tag{5.2}$$

In order to study the initial value problem as a perturbative expansion, it proves convenient to write this self-energy in the following form:

$$\Sigma^r(\vec{k},t-t') = \frac{\partial}{\partial t'} F(t-t',\vec{k}),$$

$$F(t-t',\vec{k}) = \frac{1}{\pi}\int \frac{d\omega}{\omega} \mathrm{Im}\,\widetilde{\Sigma}(\omega,\vec{k}) e^{-i\omega(t-t')}. \tag{5.3}$$

Using the form of the self-energy given by Eq. (3.17) we see that the function F can be written as

$$F(t-t',\vec{k}) = \frac{1}{2}[\mathcal{P}_+(\vec{k}) F_-(t-t',\vec{k}) + \mathcal{P}_-(\vec{k}) F_+(t-t',\vec{k})],$$

$$F_\pm(t-t',\vec{k}) = \frac{1}{\pi}\int \frac{d\omega}{\omega} \mathrm{Im}\,\widetilde{\Sigma}_\pm(\omega,\vec{k}) e^{-i\omega(t-t')}. \tag{5.4}$$

We now integrate by parts the nonlocal term in Eq. (5.1) and use the fact that the adiabatic switching-on of the external Grassman current leads to a vanishing time derivative for the fermionic expectation value for $t<0$ [38]. Upon switching off the external current at $t=0$ the effective Dirac equation of motion for the induced expectation value for $t>0$ becomes

$$\left(i\gamma_0 \frac{\partial}{\partial t} - \boldsymbol{\gamma}\cdot\vec{k} \right) \psi(\vec{k},t) + F(0,\vec{k})\psi(\vec{k},t) - \int_0^t dt' \;\; F(t-t',\vec{k}) \;\; \dot{\psi}(\vec{k},t') = 0. \tag{5.5}$$

A perturbative expansion of this equation is obtained by writing

$$F(t,\vec{k}) = g^2 F^{(2)}(t,\vec{k}) + g^4 F^{(4)}(t,\vec{k}) + \cdots,$$

$$\psi(\vec{k},t) = \psi^{(0)}(\vec{k},t) + g^2\psi^{(2)}(\vec{k},t) + g^4\psi^{(4)}(\vec{k},t) + \cdots. \tag{5.6}$$

Replacing these expansions in Eq. (5.5) leads to a hierarchy of equations, the first two terms of which are given by

$$\left(i\gamma_0 \frac{\partial}{\partial t} - \boldsymbol{\gamma}\cdot\vec{k} \right) \psi^{(0)}(\vec{k},t) = 0, \tag{5.7}$$

$$\left(i\gamma_0 \frac{\partial}{\partial t} - \boldsymbol{\gamma}\cdot\vec{k} \right) \psi^{(2)}(\vec{k},t) = -F^{(2)}(0,\vec{k})\psi^{(0)}(\vec{k},t) + \int_0^t dt' \;\; F^{(2)} \times (t-t',\vec{k}) \;\; \dot{\psi}^{(0)}(\vec{k},t'). \tag{5.8}$$

The solution of the zeroth order equation (5.7) is given by

$$\psi^{(0)}(\vec{k},t) = \sum_s \; [B^{(0)}_{\vec{k},s} U^s(\vec{k}) e^{-ikt} + D^{*(0)}_{\vec{k},s} V^s(-\vec{k}) e^{ikt}], \tag{5.9}$$

while the second order equation (5.8) can be solved in terms of the retarded free field Green's function

$$\mathcal{S}(\vec{k},t-t') = -\frac{i}{2}[\mathcal{P}_-(\vec{k}) e^{-ik(t-t')} + \mathcal{P}_+(\vec{k}) e^{ik(t-t')}]\Theta(t-t') \tag{5.10}$$

by proposing the form

$$\psi^{(2)}(\vec{k},t) = \sum_s \; [B^{(2)}_{\vec{k},s}(t) U^s(\vec{k}) e^{-ikt} + D^{*(2)}_{\vec{k},s}(t) V^s(-\vec{k}) e^{ikt}], \tag{5.11}$$

with the coefficients $B^{(2)}_{\vec{k},s}(t)$, $D^{*(2)}_{\vec{k},s}(t)$ being *slowly time dependent*. We focus on the time evolution of an initial state of particles near the Fermi surface; i.e., we set $D^{*(0)}_{\vec{k},s}=0$ and $k\approx k_F$. A straightforward computation leads to the following result:

$$B^{(2)}_{\vec{k},s}(t) = B^{(2,a)}_{\vec{k},s}(t) + B^{(2,b)}_{\vec{k},s}(t),$$

$$B^{(2,a)}_{\vec{k},s}(t) = iB^{(0)}_{\vec{k},s}\left[t\frac{1}{\pi}\int \frac{d\omega}{\omega} \;\; \mathrm{Im} \;\; \widetilde{\Sigma}_-(\omega,\vec{k}) + \frac{k}{\pi}\int \frac{d\omega}{\omega} \;\; \mathrm{Im} \;\; \widetilde{\Sigma}_-(\omega,\vec{k}) \frac{1}{(\omega-k)} \times \left(t - \frac{\sin[(\omega-k)t]}{(\omega-k)} \right) \right], \tag{5.12}$$

$$B^{(2,b)}_{\vec{k},s}(t)=B^{(0)}_{\vec{k},s}\Bigg[-\frac{k}{\pi}\int\frac{d\omega}{\omega}\times \mathrm{Im}\ \ \tilde{\Sigma}_-(\omega,\vec{k})\frac{1-\cos[(\omega-k)t]}{(\omega-k)^2}\Bigg]. \quad (5.13)$$

Using the formulas in the Appendix of Ref. [38], we find that in the limit $t\to\infty$ the two terms in Eq. (5.12) can be combined to yield

$$B^{(2,a)}_{\vec{k},s}(t)=iB^{(0)}_{\vec{k},s}t\ \ \mathrm{Re}\ \ \tilde{\Sigma}_-(\omega=k,\vec{k}). \quad (5.14)$$

The contribution $B^{(2,b)}_{\vec{k},s}(t)$ in the $t\to\infty$ and $k\approx\mu$ can be understood by writing the integral in Eq. (5.13) as follows:

$$I=-\frac{1}{\pi}\int_{-M}^{M}d\tilde{\omega}\ \ \mathrm{Im}\ \ \tilde{\Sigma}_-(\tilde{\omega},\tilde{k})\frac{1-\cos[(\tilde{\omega}-\tilde{k})t]}{(\tilde{\omega}-\tilde{k})^2},$$

$$\tilde{\omega}=\omega-\mu,\ \ \tilde{k}=k-\mu. \quad (5.15)$$

Using the formulas found in the Appendix of Ref. [38] we find for $\tilde{k}\ll M$ and $Mt\gg 1$ that

$$B^{(2,b)}_{\vec{k},s}(t)=B^{(0)}_{\vec{k},s}[-\Gamma_k t-2\lambda\ln(\bar{M}t)], \quad (5.16)$$

$$\Gamma_k=\pi\lambda\ \ |\tilde{k}|=\mathrm{Im}\ \ \tilde{\Sigma}_-(\tilde{\omega}=\tilde{k}), \quad (5.17)$$

$$\lambda=\frac{g^2}{24\pi^2},\quad \bar{M}=Me^{\gamma}, \quad (5.18)$$

and combining the above results leads to the final lowest order perturbative result:

$$B^{(2)}_{\vec{k},s}(t)=B^{(0)}_{\vec{k},s}[-i\delta_k t-\Gamma_k t-2\lambda\ln(\bar{M}t)], \quad (5.19)$$

$$\delta_k=2\lambda\tilde{k}\ln\left|\frac{\tilde{k}}{M}\right|=-\mathrm{Re}\ \ \tilde{\Sigma}_-(\tilde{\omega}=\tilde{k}), \quad (5.20)$$

with $\tilde{\Sigma}_-(\tilde{\omega})$ given by Eq. (4.30) and γ is the Euler-Mascheroni constant. We note that the damping rate Γ_k given by Eq. (5.17) coincides with the result obtained in Ref. [35], but the logarithmic term is a novel result of our analysis and is the dominant contribution for particles at the Fermi surface.

Then up to second order we find that the coefficient of the positive energy spinors in the expectation value of the spinor field is given by

$$B_{\vec{k},s}(t)=B^{(0)}_{\vec{k},s}[1-i\delta_k t-\Gamma_k t-2\lambda\ln(\bar{M}t)]. \quad (5.21)$$

The linear and logarithmic secular terms in the solution invalidate the perturbative expansion at very long times. The dynamical renormalization group introduces a systematic resummation of these secular terms as described in [38]. The implementation of the dynamical renormalization group begins by recognizing that the terms in the square brackets in Eq. (5.21) can be interpreted as a renormalization of the coefficient $B^{(0)}_{\vec{k},s}$. Thus following the procedure detailed in [38] we introduce the renormalization constant $\mathcal{Z}(\tau)$ in the form

$$B^{(0)}_{\vec{k},s}=B_{\vec{k},s}(\tau)\mathcal{Z}(\tau),\quad \mathcal{Z}(\tau)=1+\lambda z_1(\tau)+\cdots, \quad (5.22)$$

with τ an arbitrary time scale. The coefficient $z_1(\tau)$ is chosen to cancel the secular terms at the time scale $t=\tau$. Choosing this scale so that the perturbative expansion is still valid we find that the improved solution is given by

$$B_{\vec{k},s}(t)=B_{\vec{k},s}(\tau)\left[1-i\delta_k(t-\tau)-\Gamma_k(t-\tau)-2\lambda\ln\left(\frac{t}{\tau}\right)\right]. \quad (5.23)$$

Since the scale τ is arbitrary, the invariance of the solution on the choice of this scale, i.e.,

$$\frac{dB_{\vec{k},s}(t)}{d\tau}=0, \quad (5.24)$$

leads to the dynamical renormalization group equation, which to order λ is given by

$$\frac{\partial B_{\vec{k},s}(\tau)}{\partial\tau}+B_{\vec{k},s}(\tau)\left[i\delta_k+\Gamma_k+\frac{2\lambda}{\tau}\right]=0. \quad (5.25)$$

Finally we choose the arbitrary scale τ to coincide with t in the solution of Eq. (5.25) [38], leading to the renormalization group improved time-dependent amplitude

$$B_{\vec{k},s}(t)=B_{\vec{k},s}(t_0)e^{-i\delta_k(t-t_0)}e^{-\Gamma_k(t-t_0)}\left[\frac{t_0}{t}\right]^{2\lambda}. \quad (5.26)$$

Therefore the time evolution of the wave function of quasiparticle states near the Fermi surface is given by

$$\psi_{k\approx k_F}(t)=\psi_{k\approx k_F}(t_0)e^{-i(k+\delta_k)(t-t_0)}e^{-\Gamma_k(t-t_0)}\left[\frac{t_0}{t}\right]^{2\lambda}. \quad (5.27)$$

We see that the oscillation frequency $k+\delta_k$ coincides with the quasiparticle dispersion relation (4.68) to lowest order in λ while the ''damping rate'' Γ_k coincides with the quasiparticle width (4.72) to lowest order in λ. The novel aspect is the power law relaxation with anomalous dimension which cannot be extracted by computing the damping rate in an equilibrium formulation. Thus we are led to one of the important results of this article: quasiparticle excitations with the Fermi momentum relax with a power law with an anomalous dimension.

B. Time evolution from the resummed spectral density

1. $\tilde{k}=0$

We now use the renormalization group improved form of the propagator for particles near the Fermi surface to obtain the real time evolution from the inverse Fourier transform of

Eq. (3.18). An initial value problem is obtained by introducing an adiabatically switched-on external Grassman source that vanishes at $t=0$ whose Fourier transform is given by

$$\tilde{\eta}(\omega,k)=\frac{k\gamma^0}{\omega-i0^+}\sum_s\,[B_{\vec{k},s}U^s(\vec{k})-D^*_{\vec{k},s}V^s(-\vec{k})]. \tag{5.28}$$

An initial particle state is prepared by choosing $D_{\vec{k},s}=0$ with $\mathcal{P}_-(\vec{k})\tilde{\eta}(\omega,k)=2\gamma^0\tilde{\eta}(\omega,k)$. The Fourier transform is obtained by writing $e^{-i\omega t}=e^{-i\mu t}e^{-i\tilde{\omega}t}$ and performing the analytic continuation (4.37). For $k=\mu$ the long time behavior is dominated by the region $K\approx 0$ for which the analytically continued propagator is given by Eq. (4.47); we find

$$\begin{aligned}\psi(\vec{k},t) &\overset{kt\gg 1}{=} \sum_s B_{\vec{k},s}\;\; U^s(\vec{k})\;\; e^{-i\mu t}\\ &\times\int_{-i\infty+0}^{+i\infty+0}\frac{dK}{2\pi i M}\;\; e^{Kt}\;\left(\frac{K}{M}\right)^{2\lambda-1}\\ &=\psi(\vec{k},0)\;\;\frac{e^{-i\mu t}}{2\pi}\,\frac{\Gamma(2\lambda)\;\;\sin(2\pi\lambda)}{(Mt)^{2\lambda}}.\end{aligned} \tag{5.29}$$

The power law can be extracted by a simple scaling of the integration variable $K=z/t$ and is clearly a consequence of the anomalous scaling behavior of the propagator. Thus the time evolution obtained directly from the Fourier transform of the (Euclidean) renormalization group improved propagator confirms the result from the dynamical (real-time) renormalization group for excitations with Fermi momentum ($\tilde{k}=0$) and relates the power law falloff to the anomalous scaling dimension.

2. $\tilde{k}\neq 0$

The Fourier transform with the improved propagator (4.66) is more complicated because of the branch cut and the complex pole. Although obtaining an exact expression for the full integral is a complicated task, we can confirm the exponential relaxation in the narrow width approximation (weak coupling) from the contribution from the complex pole (4.75), the real and imaginary parts of which are given by Eqs. (4.68) and (4.72), respectively, in the narrow width approximation. Keeping only the contribution of the complex pole to the Fourier transform for $\tilde{k}\neq 0$ we find

$$\psi(\vec{k},t)\overset{kt\gg 1}{\approx}\psi(\vec{k},0)e^{-i\mu t}e^{-i\tilde{\omega}_p(\tilde{k})t}e^{-\Gamma(\tilde{k})t}. \tag{5.30}$$

The exponential relaxation confirms the result of the dynamical renormalization group since the narrow width approximation implies $\lambda\ll 1$ for which the power law arising from the cut contribution is subleading.

Thus the study of both cases $\tilde{k}=0$ and $\tilde{k}\neq 0$ via the Fourier transform of the renormalization group improved propagator confirms the results obtained directly in real time via the dynamical renormalization group. As was emphasized above, the most important novel feature is the power law relaxation with anomalous dimension for quasiparticles with Fermi momentum as well as the anomalous scaling dimension for the quasiparticle dispersion relation, width, and residue.

VI. FROM QED TO QCD

Although we have focused our calculations on the case of QED, it is straightforward to extrapolate the results to QCD to the same order in the HDL approximation. The reason is that the polarization tensor for gluons (photons) to this order is given by the quark loop. In the cold non-Abelian theory, the gluons give only the vacuum contribution while the quarks dominate the polarization tensor for large density. This is unlike the case at finite temperature where the gluon loops give a contribution of the same order as that of the quark loop. Furthermore, again unlike finite temperature, a magnetic gluon mass is *not* expected to arise because the gluons do not have any infrared divergence. The important changes that are required to extrapolate the results from QED to QCD are the following:

(a) The gluon mass scale (4.27) that enters in the longitudinal and transverse spectral densities (4.26) and (4.25), respectively, now becomes

$$M^2_{QCD}=\frac{g^2\mu^2}{4\pi^2}\left(\frac{N_F}{2}\right),$$

with N_F the number of flavors of quarks in the fundamental representation.

(b) The effective coupling in the self-energy of the quark now includes the trace over the color matrices resulting in that, for QCD,

$$\lambda_{QCD}=\frac{g^2}{24\pi^2}\,\frac{N_c^2-1}{2N_c}.$$

Thus the results obtained for QED to leading order in the HDL approximation can be extrapolated to QCD via the replacement $M\to M_{QCD}$, $\lambda\to\lambda_{QCD}$.

Vertex corrections: An important question that must be addressed is that of vertex corrections. In leading order in HDLs, QCD and QED are similar because the quark loop gives the leading contribution to the vector boson polarization tensor; therefore the only relevant vertex is Abelian. Since the vertex is related to the self-energy by the Ward identity, one would expect logarithmic corrections arising from the vertex. However, the results obtained from a detailed study in [27] show that this is not the case. The basic point of the argument is the following: the small momentum limit of the vertex, which is the relevant limit for long wavelength gluons, is related to the quark self-energy as

$$\Gamma^\mu(q\approx 0)=\frac{\partial\Sigma(p)}{\partial p_\mu}. \tag{6.1}$$

Since the leading behavior near the Fermi surface is

$$\Sigma(\omega,k)\propto(\omega-\mu)\ln|\omega-\mu|, \tag{6.2}$$

only the time component of the vertex would in principle lead to an infrared divergence; however, this vertex corresponds to the exchange of a longitudinal gluon which is Debye screened and does not lead to an infrared divergence. The spatial components of the vertex are infrared finite, and do not change the leading infrared divergence.

The main conclusion extracted from this argument and based on the detailed analysis of reference [27] (to which we refer the reader) is that the infrared divergences in leading order in HDLs *do not receive vertex corrections*. Hence we expect that the resummation of the leading infrared divergences provided by the renormalization group either Euclidean or in real time do not receive vertex corrections.

VII. CONCLUSIONS AND CONJECTURES

Our goal in this article is a systematic study of the breakdown of the Fermi liquid description of the *normal* state of cold and dense QED and QCD. As was recognized before, the exchange of magnetic gluons and photons that are only dynamically screened by Landau damping leads to infrared divergences in the quark self-energy for particles near the Fermi surface. The main aspect of this article is the recognition that these divergences are akin to those arising in a critical theory near its upper critical dimensionality. We then implemented both the Euclidean and the dynamical renormalization group to provide a nonperturbative resummation of the leading infrared singularities to analyze equilibrium and nonequilibrium aspects of the single (quasi)particle states near the Fermi surface. The non-perturbative resummation of the single particle propagator leads to a novel description of the spectrum of quasiparticle excitations with momentum near the Fermi momentum summarized as follows

(i) The quasiparticle pole, width, and residue (wave function renormalization) are given by

$$\tilde{\omega}_p(\tilde{k})=\mathrm{sgn}(\tilde{k})[|\tilde{k}|M^{-2\lambda}\cos(\pi\lambda)]^{1/(1-2\lambda)},$$

$$\Gamma(\tilde{k})=Z_p[\tilde{k}]|\tilde{k}|\sin[\pi\lambda],$$

$$Z_p[\tilde{k}]=\frac{\left|\frac{\tilde{\omega}_p(\tilde{k})}{M}\right|^{2\lambda}}{(1-2\lambda)},$$

$$\tilde{\omega}=\omega-k_F,\quad \tilde{k}=k-k_F,$$

respectively. Therefore the residue of the ''quasiparticle pole'' and the ''quasiparticle width'' vanishes near the Fermi surface as

$$Z_p[\tilde{k}]\propto|k-k_F|^{2\lambda/(1-2\lambda)}, \tag{7.1}$$

$$\Gamma(\tilde{k})\propto|k-k_F|^{1/(1-2\lambda)}, \tag{7.2}$$

and the group velocity of quasiparticles with Fermi momentum vanishes, indicating a collective backflow.

The real-time evolution of the single quasiparticle wave function for states near the Fermi momentum is given by

$$\psi_{k\approx k_F}(t)\approx\psi_{k\approx k_F}(t_0)e^{-i[k_F+\tilde{\omega}_p(\tilde{k})](t-t_0)}e^{-\Gamma(\tilde{k})(t-t_0)}\left[\frac{t_0}{t}\right]^{2\lambda}. \tag{7.3}$$

Therefore quasiparticles with the Fermi momentum relax with a power law determined by the anomalous scaling dimension, revealing that the physics near the Fermi surface is similar to that of a critical theory.

(ii) The single quasiparticle distribution function is *continuous* near the Fermi momentum; i.e., the ''jump'' discontinuity in the Fermi-Dirac distribution vanishes as a consequence of the vanishing of the quasiparticle residue at the Fermi momentum. We find

$$n_{k\approx k_F}=\frac{\sin[\pi\lambda]}{2\pi\lambda}-\frac{(k-k_F)}{\pi M(1-4\lambda)}+\mathcal{O}(k-k_F)^2. \tag{7.4}$$

The vanishing of the discontinuity of the distribution function at the Fermi surface is the hallmark of the breakdown of Fermi liquid theory.

There are some remarkable similarities between these features of cold dense QCD and QED and those of quasi-one-dimensional Fermi systems with marginal interactions that lead to a description as Luttinger liquids [39,40]. These systems also feature spectral densities and correlation functions with anomalous dimensions which are nonuniversal and depend on the couplings [39,40]. The fermion propagator that results from one gluon exchange (dynamically screened) is also similar to that conjectured to describe the normal phase of high temperature superconductors in terms of marginal Fermi liquids [48,49]. Even if these similarities are just coincidental, it is possible that a body of results in the condensed matter literature could be useful to understand the fundamental aspects of the normal phase of QCD at high density.

Potential impact of the results. As we mentioned in the Introduction, the properties of the normal state not only determine the thermodynamics and transport properties but also influence those of the superconducting state, since superconductivity appears as an instability of the normal state towards pairing interactions. Therefore the results obtained in this article that pertain solely to the normal phase could bear on characteristics of the superconducting state as well as transport in the normal (and possible in the superconducting) phase.

(i) In Ref. [27] it was found that the same type of infrared divergences that lead to the breakdown of Fermi liquid theory are responsible for a substantial decrease of the superconducting gap. In the calculation of Ref. [27], these divergences are manifest through the wave function renormalization in the equation for the gap. Furthermore, recently lifetime effects (of the normal state quasiparticles) were shown to lead to a further decrease of the superconducting gap [31]. In this article we have shown how the wave function renormalization logarithmic divergence sums up to produce anomalous dimensions, which change the quasiparticle

description. The spectral density features anomalous dimensions for frequency and momenta near the putative Fermi surface as well as important modifications in the quasiparticle dispersion relations, lifetimes, and residues. It is therefore a relevant question to assess the potential corrections of the resummed spectral densities for the normal quark propagators to the superconducting gap. This entails solving the gap equation or alternatively the Dyson-Schwinger equation but with the normal quark propagators replaced by those obtained from the resummed spectral functions. We are currently studying this possibility and expect to report on our findings in the near future.

(ii) As mentioned in the Introduction the most relevant physical setting for cold and dense QCD is that of astrophysical compact objects, in particular protoneutron stars from type II supernova collapse or neutron stars (or pulsars). An important observational aspect that could yield information from the core of neutron stars is cooling, which is studied through (soft) x-ray emmision [50]. The cooling equation

$$\frac{dE}{dt}=C\frac{dT}{dt}=-[L_\nu+L_\gamma]$$

relates the neutrino and photon luminosities to the specific heat C. For normal quark matter the neutrino emissivity is dominated by the direct quark Urca processes $d\to u\ e\ \overline{\nu}$, $u\ e\to d\,\nu$ [51]. A *normal* weakly interacting degenerate Fermi gas has a typical specific heat linear in temperature $C(T)=C_0T$ where the coefficient C_0 depends on the Fermi liquid properties. In particular the wave function renormalization (residue at the quasiparticle pole) renormalizes the free field (free Fermi gas) value of C_0. Since the quasiparticle residue vanishes, signaling the breakdown of Fermi liquid theory, we *conjecture* that the linear law will be replaced in a manner similar to that of Kondo-type systems [42], $C\propto\ln(T)$. If a superconducting instability introduces a gap for all quarks, then the specific heat will have a typical behavior $C_1\ e^{-\Delta(T)/T}$ (for $T<T_c$) where $\Delta(T)$ is the superconducting gap and C_1 depends on the density of quasiparticle states near the Fermi surface which again receives non-Fermi-liquid renormalization corrections. If the neutrino and photon emissivity of quarks is suppressed because of the presence of a superconducting gap, then the electronic specific heat will become relevant, in which case again the non-Fermi-liquid corrections to the specific heat will be important since there are no superconducting pairing instabilities in QED. If some of the quarks are ungapped, these are *normal* and will receive renormalization of their Fermi liquid behavior.

Understanding the potential corrections of the breakdown of Fermi liquid theory both for quarks and leptons could therefore lead to a deeper understanding of cooling in neutron stars and therefore justifies further studies along these lines.

Our analysis was based on a perturbative approach; therefore its range of validity is restricted to asymptotically large densities so that the effective coupling $\alpha_s(\mu)/6\pi\ll 1$. Using the running of the QCD coupling constant, the weak coupling condition implies chemical potentials and baryon densities orders of magnitude larger than those available at the core of neutron stars. Thus our studies for the properties of the normal phase, along with those of color superconductivity, must be taken as indicative of novel and potentially relevant phenomena, but must be carefully extrapolated to the realm of the baryochemical potential (baryon density) relevant to quark matter in neutron stars, requiring alternative nonperturbative techniques.

ACKNOWLEDGMENTS

D.B. thanks the NSF for support through grants PHY-9605186, PHY-9988720, and CNRS-NSF-INT-9815064. H.J.d.V. thanks CNRS for support through a binational collaboration. The authors thank R. Pisarski and D. Rischke for fruitful discussions. D.B. thanks D. Jasnow, K. Rajagopal, M. Stephanov, D. Blaschke, F. Weber, C. Roberts, and S. Schmidt for illuminating discussions and comments.

APPENDIX: REAL-TIME PROPAGATORS

1. Dirac fields

In this appendix we summarize the various real-time propagators used in this article. The fermion propagators are defined by

$$\langle\Psi^a(\vec{x},t)\overline{\Psi}^b(\vec{x}',t')\rangle=i\int\frac{d^3k}{(2\pi)^3}S^{ab}_{\vec{k}}(t,t')\,e^{i\vec{k}\cdot(\vec{x}-\vec{x}')},$$

$$S^{++}_{\vec{k}}(t,t')=S^{>}_{\vec{k}}(t,t')\,\theta(t-t')+S^{<}_{\vec{k}}(t,t')\,\theta(t'-t),$$

$$S^{--}_{\vec{k}}(t,t')=S^{>}_{\vec{k}}(t,t')\,\theta(t'-t)+S^{<}_{\vec{k}}(t,t')\,\theta(t-t'),$$

$$S^{\pm\mp}_{\vec{k}}(t,t')=S^{\lessgtr}_{\vec{k}}(t,t'),\tag{A1}$$

where $a,\ b=\pm$.

In an equilibrium situation the propagators can be written in terms of spectral densities as follows:

$$iS^{>}_{\vec{k}}(t,t')=\int dq_0\,\rho^{>}(q_0,\vec{k})e^{-iq_0(t-t')},$$

$$-iS^{<}_{\vec{k}}(t,t')=\int dq_0\,\rho^{<}(q_0,\vec{k})e^{-iq_0(t-t')},$$

$$\rho^{>}(q_0,\vec{k})=\rho(q_0,\vec{k})[1-N_f(q_0,k)],$$

$$\rho^{<}(q_0,\vec{k})=\rho(q_0,\vec{k})N_f(q_0,k),\tag{A2}$$

where the Fermi-Dirac distribution functions for particles and antiparticles, for the case under consideration of finite chemical potential μ and zero temperature, are given by

$$N_f(q_0)=\Theta(\mu-q_0),\tag{A3}$$

$$\overline{N}_f(q_0)=\Theta(-\mu-q_0).\tag{A4}$$

For free fields the fermion Wightman functions are given by

$$S^{>}_{\vec{k}}(t,t') = -\frac{i}{2\omega_{\vec{k}}}\{(\not{K}+m)[1-N_F(\omega_{\vec{k}})]e^{-i\omega_{\vec{k}}(t-t')} + \gamma_0(\not{K}-m)\gamma_0\,\overline{N}_F(\omega_{\vec{k}})\,e^{i\omega_{\vec{k}}(t-t')}\},$$

$$S^{<}_{\vec{k}}(t,t') = \frac{i}{2\omega_{\vec{k}}}\{(\not{K}+m)\,N_F(\omega_{\vec{k}})\,e^{-i\omega_{\vec{k}}(t-t')} + \gamma_0(\not{K}-m)\gamma_0[1-\overline{N}_F(\omega_{\vec{k}})]e^{i\omega_{\vec{k}}(t-t')}\}, \tag{A5}$$

with $K=(\omega_{\vec{k}},\vec{k})$, $\not{K}=\gamma^0\omega_{\vec{k}}-\vec{\gamma}\cdot\vec{k}$, and $\omega_{\vec{k}}=\sqrt{\vec{k}^2+m^2}$. For massless fermions (the case under consideration),

$$\left\{\frac{(\not{K}+m)}{\omega_{\vec{k}}}\right\}_{m=0} = \mathcal{P}_-(\hat{\vec{k}}) = \gamma^0-\vec{\gamma}\cdot\hat{\vec{k}},$$

$$\left\{\frac{\gamma_0(\not{K}-m)\gamma_0}{\omega_{\vec{k}}}\right\}_{m=0} = \mathcal{P}_+(\hat{\vec{k}}) = \gamma^0+\vec{\gamma}\cdot\hat{\vec{k}}, \tag{A6}$$

with the properties

$$(\mathcal{P}_-(\hat{\vec{k}}))^2=(\mathcal{P}_+(\hat{\vec{k}}))^2=0,$$

$$\mathcal{P}_-(\hat{\vec{k}})\mathcal{P}_+(\hat{\vec{k}})=2\gamma^0\mathcal{P}_+(\hat{\vec{k}}),$$

$$\mathcal{P}_+(\hat{\vec{k}})\mathcal{P}_-(\hat{\vec{k}})=2\gamma^0\mathcal{P}_-(\hat{\vec{k}}). \tag{A7}$$

2. Gauge fields

a. Spatial components

The transverse photon propagators are defined by

$$\langle A^{i,a}_T(\vec{x},t)A^{j,b}_T(\vec{x}',t')\rangle = -i\int\frac{d^3q}{(2\pi)^3}\mathcal{G}^{ab}_{T,q}(t,t')\times\mathcal{P}^{ij}_T(\vec{q})\,e^{i\vec{q}\cdot(\vec{x}-\vec{x}')},$$

$$\mathcal{G}^{++}_{T,q}(t,t') = \mathcal{G}^{>}_{T,q}(t,t')\,\theta(t-t') + \mathcal{G}^{<}_{T,q}(t,t')\,\theta(t'-t),$$

$$\mathcal{G}^{--}_{T,q}(t,t') = \mathcal{G}^{>}_{T,q}(t,t')\,\theta(t'-t) + \mathcal{G}^{<}_{T,q}(t,t')\,\theta(t-t'),$$

$$\mathcal{G}^{\pm\mp}_{T,q}(t,t') = \mathcal{G}^{\gtrless}_{T,q}(t,t'), \tag{A8}$$

where $\mathcal{P}^{ij}_T(\vec{q})=\delta^{ij}-\hat{q}^i\hat{q}^j$ is the transverse projector and the photon Wightman functions can be written in terms of a spectral representation as follows:

$$\mathcal{G}^{>}_{T,q}(t,t') = i\int dq_0\,\tilde{\rho}_T(q_0,q)\,[1+n_B(q_0)]\,e^{-iq_0(t-t')},$$

$$\mathcal{G}^{<}_{T,q}(t,t') = i\int dq_0\,\tilde{\rho}_T(q_0,q)\,n_B(q_0)\,e^{-iq_0(t-t')}, \tag{A9}$$

where $\tilde{\rho}_T(q_0,q)$ is the spectral density and $n_B(q_0)$ is the Bose-Einstein distribution function.

At zero temperature

$$n_B(q_0)=-\Theta(-q_0), \quad 1+n_B(q_0)=\Theta(q_0). \tag{A10}$$

For free fields at zero temperature we find

$$\mathcal{G}^{>}_{T,q}(t,t') = \frac{i}{2q}e^{-iq(t-t')},$$

$$\mathcal{G}^{<}_{T,q}(t,t') = \frac{i}{2q}e^{iq(t-t')}. \tag{A11}$$

In the HDL approximation, the spectral density $\tilde{\rho}_T(q_0,q)$ is given by

$$\tilde{\rho}_T(q_0,q)=\mathrm{sgn}(q_0)\,Z_T(q)\,\delta[q_0^2-\omega_T^2(q)]+\beta_T(q_0,q)\;\;\theta(q^2-q_0^2),$$

$$\beta_T(\omega,k)=\frac{\dfrac{g^2\mu^2}{4\pi^2}\dfrac{\omega}{k}\left(1-\dfrac{\omega^2}{k^2}\right)}{\left\{\omega^2-k^2-\dfrac{g^2\mu^2}{4\pi^2}\left[\dfrac{2\omega^2}{k^2}+\dfrac{\omega}{k}\left(1-\dfrac{\omega^2}{k^2}\right)\ln\left|\dfrac{k+\omega}{k-\omega}\right|\right]\right\}^2+\left[\dfrac{g^2\mu^2}{4\pi}\dfrac{\omega}{k}\left(1-\dfrac{\omega^2}{k^2}\right)\right]^2}, \tag{A12}$$

and $Z_T(q)$ is the residue at the pole of the collective excitation [33].

b. Time component of the photon propagator

The time-time component of the photon propagator describes the instantaneous Coulomb interaction including screening corrections and is given by

$$\langle A_0^a(\vec{x},t)A_0^b(\vec{x}',t')\rangle = i\int \frac{d^3q}{(2\pi)^3}\mathcal{G}^{ab}_{L,q}(t,t')e^{i\vec{q}\cdot(\vec{x}-\vec{x}')},$$

$$\mathcal{G}^{++}_{L,q}(t,t') = \frac{1}{q^2}\delta(t-t') + \mathcal{G}^{>}_{L,q}(t,t')\,\theta(t-t') + \mathcal{G}^{<}_{L,q}(t,t')\,\theta(t'-t),$$

$$\mathcal{G}^{--}_{L,q}(t,t') = -\frac{1}{q^2}\delta(t-t') + \mathcal{G}^{>}_{L,q}(t,t')\,\theta(t'-t) + \mathcal{G}^{<}_{L,q}(t,t')\,\theta(t-t'),$$

$$\mathcal{G}^{\pm\mp}_{L,q}(t,t') = \mathcal{G}^{\lessgtr}_{L,q}(t,t'), \qquad \text{(A13)}$$

with the Wightman functions expressed in terms of the spectral density $\tilde{\rho}_L$ as

$$\mathcal{G}^{>}_{L,q}(t,t') = -i\int dq_0\,\tilde{\rho}_L(q_0,q)\,[1+n_B(q_0)]\,e^{-iq_0(t-t')},$$

$$\mathcal{G}^{<}_{L,q}(t,t') = -i\int dq_0\,\tilde{\rho}_L(q_0,q)\,n_B(q_0)\,e^{-iq_0(t-t')}. \qquad \text{(A14)}$$

For free fields $\tilde{\rho}_L(q_0,q)=0$ and

$$\mathcal{G}^{++}_{L,q}(t,t') = \frac{1}{q^2}\delta(t-t'),$$

$$\mathcal{G}^{--}_{L,q}(t,t') = -\frac{1}{q^2}\delta(t-t'),$$

$$\mathcal{G}^{\pm\mp}_{L,q}(t,t') = 0. \qquad \text{(A15)}$$

In the hard dense loop approximation the spectral density $\tilde{\rho}_L(q_0,q)$ is given by

$$\tilde{\rho}_L(q_0,q) = \mathrm{sgn}(q_0)\,Z_L(q)\,\delta[q_0^2-\omega_L^2(q)] + \beta_L(q_0,q)\;\;\theta(q^2-q_0^2),$$

$$\beta_L(q_0,q) = \frac{\dfrac{g^2\mu^2}{2\pi^2}\dfrac{q_0}{q}}{\left[q^2+\dfrac{g^2\mu^2}{2\pi^2}\left(2-\dfrac{q_0}{q}\ln\left|\dfrac{q+q_0}{q-q_0}\right|\right)\right]^2+\left[\dfrac{g^2\mu^2}{2\pi}\dfrac{q_0}{q}\right]^2}, \qquad \text{(A16)}$$

where $\omega_L(q)$ is the plasmon (longitudinal photon) pole and $Z_L(q)$ is the corresponding residue [33].

[1] P. Braun-Munzinger, nucl-ex/0007021.

[2] N. K. Glendenning, *Compact Stars, Nuclear Physics, Particle Physics and General Relativity* (Springer, New York, 1997).

[3] F. Weber, *Pulsars as Astrophysical Laboratories for Nuclear and Particle Physics* (IOP, Bristol, 1999); J. Phys. G **25**, R195 (1999); Acta Phys. Pol. B **30**, 3149 (1999).

[4] N. K. Glendenning and F. Weber, ''Possible evidence of quark matter in neutron star X-ray binaries,'' astro-ph/0003426.

[5] D. Blaschke, H. Grigorian, and G. Poghosyan, ''Conditions for deconfinement transition signals from compact star rotation,'' astro-ph/0008005; E. Chubarian, H. Grigorian, G. Poghosyan, and D. Blaschke, ''Deconfinement transition in rotating compact stars,'' astro-ph/9903489.

[6] S. Hands, J. B. Kogut, M. P. Lombarde, and S. E. Morrison, Nucl. Phys. **B558**, 327 (1999).

[7] S. Hands and S. E. Morrison, Phys. Rev. D **59**, 116002 (1999).

[8] J. B. Kogut, M. A. Stephanov, D. Toublan, J. J. M. Verbaarschot, and A. Zhitnitsky, Nucl. Phys. **B582**, 477 (2000).

[9] D. Bailin and A. Love, Nucl. Phys. **B190**, 175 (1981); **B205**, 119 (1982); Phys. Rep. **107**, 325 (1984).

[10] M. Alford, K. Rajagopal, and F. Wilczek, Phys. Lett. B **422**, 247 (1998); Nucl. Phys. **B537**, 443 (1999).

[11] R. Rapp, T. Schaefer, E. V. Shuryak, and M. Velkovsky, Phys. Rev. Lett. **81**, 53 (1998); Ann. Phys. (N.Y.) **280**, 35 (2000).

[12] T. Schäfer and F. Wilczek, Phys. Rev. D **60**, 074014 (1999).

[13] J. Berges and K. Rajagopal, Nucl. Phys. **B538**, 215 (1999).

[14] D. T. Son, Phys. Rev. D **59**, 094019 (1999).

[15] R. D. Pisarski and D. H. Rischke, Phys. Rev. D **61**, 074017 (2000); **61**, 051501(R) (2000); **60**, 094013 (1999).

[16] D. H. Rischke, Phys. Rev. D **62**, 054017 (2000); **62**, 034007 (2000).

[17] W. E. Brown, J. T. Liu, and H-c. Ren, Phys. Rev. D **61**, 114012 (2000); **62**, 054016 (2000).

[18] D. K. Hong, V. A. Miransky, I. A. Shovkovy, and L. C. R. Wijewardhana, Phys. Rev. D **61**, 056001 (2000).

[19] B.-Y. Park, M. Rho, A. Wirzba, and I. Zahed, Phys. Rev. D **62**, 034015 (2000).

[20] For reviews, see F. Wilczek, ''QCD in Extreme Conditions,'' hep-ph/0003183; T. Schafer, ''Color Superconductivity,'' nucl-th/9911017; K. Rajagopal, Nucl. Phys. **A661**, 150c (1999).

[21] C. D. Roberts and S. M. Schmidt, ''Dyson-Schwinger Equations: Density, Temperature and Continuum Strong QCD,'' nucl-th/0005064; J. C. R. Bloch, C. D. Roberts, and S. M. Schmidt, Phys. Rev. C **60**, 065208 (1999).
[22] D. Blaschke, T. Klahn, and D. V. Voskresensky, Astrophys. J. **533**, 406 (2000); D. Blaschke, D. M. Sedrakian, and K. M. Shahabasyan, ''Diquark condensates and the magnetic field of pulsars,'' astro-ph/9904395.
[23] G. W. Carter and S. Reddy, Phys. Rev. D **62**, 103002 (2000).
[24] D. Page, M. Prakash, J. M. Lattimer, and A. Steiner, Phys. Rev. Lett. **85**, 2048 (2000).
[25] For a recent review, see K. Rajagopal, ''The Phases of QCD in Heavy Ion Collisions and Compact Stars,'' hep-ph/0009058.
[26] C. Song, ''Dense Nuclear Matter: Landau Fermi Liquid Theory and Chiral Lagrangians with Scaling,'' nucl-th/0006030; M. Rho, ''Physics of Dense and Superdense Matter,'' nucl-th/0007073; ''Effective Field Theories, Landau-Migdal Fermi-Liquid Theory and Effective Chiral Lagrangians for Nuclear Matter,'' nucl-th/0007060.
[27] W. E. Brown, J. T. Liu, and H-c. Ren, Phys. Rev. D **62**, 054013 (2000).
[28] T. Holstein, R. E. Norton, and P. Pincus, Phys. Rev. B **8**, 2649 (1973).
[29] M. Y. Reizer, Phys. Rev. B **40**, 11 571 (1989); **44**, 5476 (1991).
[30] S. Chakravarty, R. E. Norton, and O. F. Syljuasen, Phys. Rev. Lett. **74**, 1423 (1995).
[31] C. Manuel, Phys. Rev. D **62**, 114008 (2000).
[32] E. Braaten and R. D. Pisarski, Nucl. Phys. **B337**, 569 (1990); **B339**, 310 (1990).
[33] M. Le Bellac, *Thermal Field Theory* (Cambridge University Press, Cambridge, England, 1996).
[34] J.-P. Blaizot and J.-Y. Ollitrault, Phys. Rev. D **48**, 1390 (1993).
[35] B. Vanderheyden and J.-Y. Ollitrault, Phys. Rev. D **56**, 5108 (1997).
[36] M. Le Bellac and C. Manuel, Phys. Rev. D **55**, 3215 (1997).
[37] C. Manuel, Phys. Rev. D **62**, 076009 (2000).
[38] D. Boyanovsky, H. J. de Vega, R. Holman, and M. Simionato, Phys. Rev. D **60**, 065003 (1999); D. Boyanovsky and H. J. de Vega, *ibid.* **59**, 105019 (1999); D. Boyanovsky, H.J. de Vega, and S.-Y. Wang, *ibid.* **61**, 065006 (2000); S.-Y. Wang, D. Boyanovsky, H. J. de Vega, and D.-S. Lee, *ibid.* **62**, 105026 (2000).
[39] H. J. Schulz, G. Cuniberti, and P. Pieri, ''Fermi liquids and Luttinger liquids,'' Lecture notes of the Chia Laguna, Italy, summer school, 1997, cond-mat/9807366; J. Voigt, Rep. Prog. Phys. **58**, 977 (1995).
[40] A. J. Schofield, Contemp. Phys. **40**, 95 (1999).
[41] G. Baym and C. Pethick, *Landau Fermi Liquid Theory: Concepts and Applications* (Wiley, New York, 1991).
[42] G. Mahan, *Many Particle Physics* (Plenum, New York, 1990); S. Doniach and X. Sondheimer, *Green's Functions for Solid State Physicists* (Imperial College Press, London, 1998) [see Chap. 9 and formula (9.2.20)].
[43] J. J. Quinn and R. A. Ferrell, Phys. Rev. **112**, 812 (1958).
[44] R. Shankar, Rev. Mod. Phys. **66**, 129 (1995); J. Polchinski, in *Recent Directions in Particle Theory: From Superstrings and BlackHoles to the Standard Model*, edited by J. Harvey and J. Polchinski (World Scientific, Singapore, 1994).
[45] J. R. Schrieffer, *Theory of Superconductivity* (Addison-Wesley, Redwood City, CA, 1964).
[46] N. Evans, S. D. H. Hsu, and M. Schwetz, Nucl. Phys. **B551**, 275 (1995); S. D. H. Hsu and M. Schwetz, *ibid.* **B572**, 211 (2000).
[47] E. Daniel and S. H. Vosko, Phys. Rev. **120**, 2041 (1960).
[48] C. M. Varma, P. B. Littlewood, and S. Schmitt-Rink, Phys. Rev. Lett. **63**, 1996 (1989).
[49] P. W. Anderson, Phys. Rev. Lett. **64**, 1839 (1990).
[50] Ch. Schaab, F. Weber, M. K. Weigel, and N. K. Glendenning, Nucl. Phys. **A605**, 531 (1996).
[51] N. Iwamoto, Ann. Phys. (N.Y.) **141**, 1 (1980).